Jak-TGFβ cross-talk links transient adipose tissue inflammation to beige adipogenesis

Committing progenitors to adipogenesis

Promoting the "browning" of white fat has been proposed as a strategy to combat obesity. Beige adipocytes, which are intermediate between fat-storing white adipocytes and thermogenic brown adipocytes, can emerge from the differentiation of adipocyte progenitors in adipose tissue in response to β_3-adrenergic stimulation. Using primary human and mouse cells and ex vivo mouse models, Babaei *et al*. (see also the Focus by Sun *et al*.) found that the Jak family of kinases promoted the commitment of adipocyte progenitors to beige adipogenesis. Through the downstream transcription factor Stat3, Jak inhibited TGFβ signaling and prevented adipocyte progenitors from differentiating into smooth muscle cells. β_3-Adrenergic stimulation of lipolysis, which transiently triggers inflammation, induced the production of the cytokines IL-6 and IL-11, which activated the Jak/Stat3 pathway. These results delineate a pathway that is activated by transient inflammation in adipose tissue that steers adipocyte progenitors toward differentiation into a thermogenically active form of fat.

Abstract

The transient activation of inflammatory networks is required for adipose tissue remodeling including the "browning" of white fat in response to stimuli such as β3-adrenergic receptor activation. In this process, white adipose tissue acquires thermogenic characteristics through the recruitment of so-called beige adipocytes. We investigated the downstream signaling pathways impinging on adipocyte progenitors that promote de novo formation of adipocytes. We showed that the Jak family of kinases controlled TGFβ signaling in the adipose tissue microenvironment through Stat3 and thereby adipogenic commitment, a function that was required for beige adipocyte differentiation of murine and human progenitors. Jak/Stat3 inhibited TGFβ signaling to the transcription factors Srf and Smad3 by repressing local *Tgfb3* and *Tgfb1* expression before the core transcriptional adipogenic cascade was activated. This pathway cross-talk was triggered in stromal cells by ATGL-dependent adipocyte lipolysis and a transient wave of IL-6 family cytokines at the onset of adipose tissue remodeling induced by β3-adrenergic receptor stimulation. Our results provide insight into the activation of adipocyte progenitors and are relevant for the therapeutic targeting of adipose tissue inflammatory pathways.

INTRODUCTION

Adipose tissue can undergo substantial growth or remodeling in response to environmental challenges. Fate mapping experiments have established that this plasticity depends, to a substantial extent, on the formation of new adipocytes from resident immature progenitor cells, in some cases after transient proliferation (*1*–*4*). On one hand, calorie excess can promote the generation of lipid-storing adipocytes and thereby tissue hyperplasia. On the other hand, progenitors can give rise to beige (also known as brite) adipocytes that can dissipate energy as heat through the expression and activation of uncoupling protein 1 (Ucp1) (*5*). This process contributes to browning of white fat, in which white fat acquires an oxidative and thermogenic phenotype, triggered by prolonged cold exposure, exercise, cachexia, trauma, or β-adrenergic stimulation in rodents and partially in humans (*6*–*8*).

Transient activation of innate immune cells and inflammatory mediators plays a key role in the induction of adipogenesis and thermogenic tissue remodeling in vivo (*9*–*12*). However, the mechanisms linking inflammatory signaling to adipocyte progenitor responses are largely unknown. The Janus kinase (Jak) family of receptor-associated tyrosine kinases (Jak1, Jak2, Jak3, and Tyk2) act as primary transducers of multiple cytokine receptors and mediate many of their effects through the phosphorylation of the signal transducer and activator of transcription (Stat) family of transcription factors (*13*). The Jak/Stat pathway is also involved in adipocyte differentiation [reviewed in (*14*)]. However, our knowledge on physiologically relevant upstream activators impinging on progenitor cells and downstream effectors in adipose tissue is limited.

Here, we addressed the function and mechanism of the Jak family of kinases and Stat3 in murine and human adipocyte progenitors, including their thermogenic differentiation. In contrast to previous studies on white adipocyte cell lines (*14*–*16*), we demonstrated that the primary role of the Jak family was to inhibit local transforming growth factor–β (TGFβ) signaling to enable adipogenic commitment, independently of the induction of the core adipogenic transcription factors. This cross-talk was required for beige adipocyte differentiation and was triggered by β-adrenergic lipolytic stress and interleukin-6 (IL-6) family cytokines in vivo, providing a paradigm that links local metabolic signals to progenitor cell responses and tissue remodeling.

RESULTS

Adipogenesis and particularly beige adipocyte differentiation depend on Jak activity in murine and human immature progenitors

The Jak family of kinases are broadly expressed and cooperate at multiple receptors, but due to specific critical functions, genetic deficiency results in lethal or severe phenotypes (*13*). To overcome these obstacles and to address their role in adipocyte progenitors, we used a primary cell model based on a defined progenitor population and a physiologically relevant beige differentiation inducer (*11*, *17*, *18*). In this system, $Lin^-(CD45^-CD31^-Ter119^-)Sca1^+$ cells from murine subcutaneous fat are treated with carbaprostacyclin ($cPGI_2$), the stable analog of the cyclooxygenase-generated prostaglandin (PGI_2) (*19*). This treatment leads to progenitor activation followed by beige adipocyte differentiation, which is mediated by both the prostaglandin I (IP) receptor (encoded by *Ptgir*) and peroxisome proliferator–activated receptor-γ (Pparg) (*11*, *18*). Treatment with the pan-Jak inhibitor I (JakiI) (*20*) throughout differentiation resulted in the marked dose-dependent reduction of $cPGI_2$-induced thermogenic gene expression, including *Ucp1*, *Cidea*, and the mitochondrial markers *Cpt1b*, *Cox7a1*, and *Ppargc1a*, as well as the general markers of adipogenesis *Retn*, *Fabp4*, and *Pparg* (Fig. 1A). The increase in Ucp1 protein expression by $cPGI_2$ was abolished in JakiI-treated cells even at higher $cPGI_2$ concentrations (Fig. 1, B to D, and fig. S1, A and B). This effect persisted after normalization for the reduction of adipocyte differentiation by continuous Jak inhibition (Fig. 1, B and C, and fig. S1C). Furthermore, oxygen consumption analysis revealed that the norepinephrine-induced uncoupled respiration observed in $cPGI_2$-treated beige adipocytes was substantially inhibited in cells differentiated in the presence of JakiI (Fig. 1, E and F).

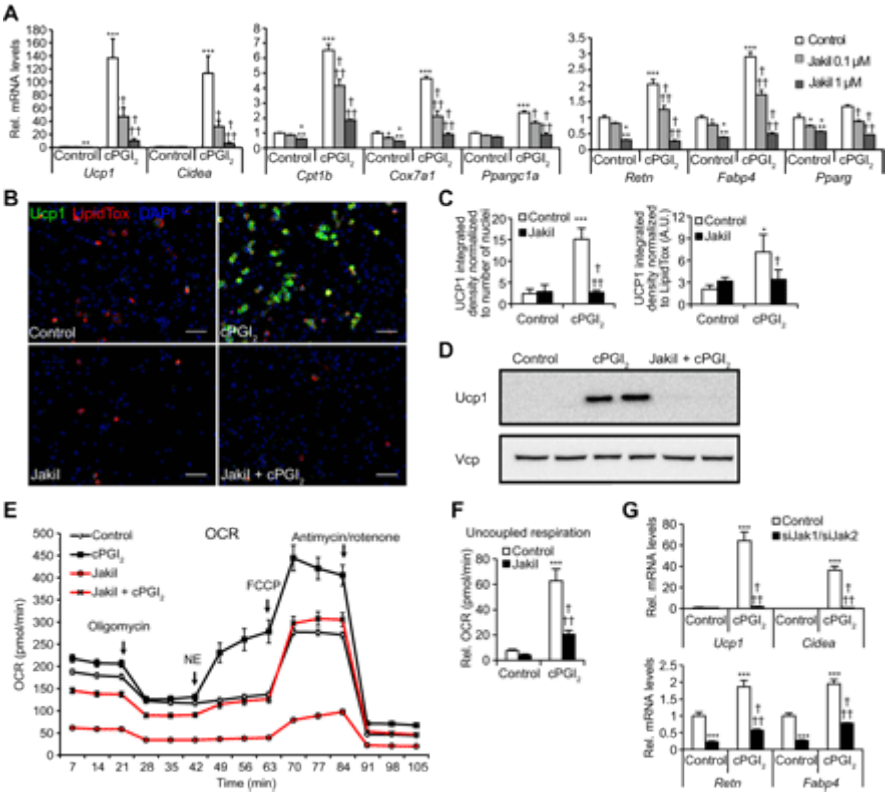

- Download high-res image
- Open in new tab
- Download Powerpoint

Fig. 1 Continuous inhibition of Jak1/2 activity disrupts white and beige adipocyte differentiation of defined murine progenitors.

(**A** to **G**) $Lin^{-}Sca1^{+}$ progenitor cells from mouse inguinal fat were subjected to 8-day differentiation in the presence of 1 μM (A to C and G) or 5 μM (D to F) $cPGI_2$ (or vehicle). Cells were treated with 0.2 μM (A to C) or 1 μM (D to F) JakiI (or vehicle) from day 0 to day 8. (A) Quantitative reverse transcription polymerase chain reaction (qRT-PCR) analysis of thermogenic, mitochondrial, and adipogenic genes. (B) Cells were costained with LipidTOX, anti-Ucp1, and 4′,6-diamidino-2-phenylindole (DAPI). Scale bars, 100 μm. (C) Quantitative image analysis of (B). (D) Representative Western blot of Ucp1, with Vcp as a loading control. Each lane represents an independent culture. (E) Representative graph of cellular respiration analysis (n = 12 independent cultures from three or more mice). OCR, oxygen consumption rate. (F) Normalized norepinephrine (NE)–induced respiration from (E). (G) qRT-PCR analysis of cells transfected with the indicated siRNAs and differentiated for 8 days. (A to C and G) n = 3 independent cultures from three or more mice. Two-way analysis of variance (ANOVA) with Bonferroni post hoc comparisons: "*" indicates the difference to control/control, and "†" indicates the difference to control between $cPGI_2$-treated groups. A.U., arbitrary units.

To validate the specificity of these findings, we replaced JakiI with the compound CP-690550, which targets Jak1, Jak2, and Jak3 (*21*), and confirmed a significant more than twofold reduction in thermogenic and adipogenic gene expression (fig. S1D). We next used combinatorial knockdown in immature progenitors to further narrow down the Jak family members responsible for this phenotype. This revealed that knockdown of only *Jak1* or *Jak2*,

but not *Tyk2* or *Jak3*, reduced expression of the Jak/Stat3 target gene *Socs3* to a degree comparable with JakiI treatment (fig. S1, E to I). *Jak1*/*Jak2* double knockdown was sufficient to potently inhibit *Ucp1*, *Cidea*, *Retn*, and *Fabp4* expression and phenocopy the effect of prolonged pharmacological Jak inhibition (Fig. 1G).

The role of the Jak family of kinases in human progenitor differentiation has not been previously addressed. To test whether the essential function observed in mouse cells was conserved in the human system, we used two models of human thermogenic adipocyte differentiation. In accordance with Ghandour *et al*. (22), $cPGI_2$ treatment during the differentiation of human multipotent adipose-derived stem cells (hMADS) caused a robust increase in thermogenic marker gene and protein expression (Fig. 2, A and B, and fig. S2). JakiI treatment abolished the induction of *UCP1*, *CIDEA*, and *FABP3*, as well as UCP1 protein expression. We sought to validate this result in freshly isolated stromal cells from human subcutaneous fat [human stromal vascular fraction (hSVF)], which contain adipocyte progenitors. The $cPGI_2$-induced expression of *UCP1* and *CPT1B* was significantly suppressed by JakiI treatment (Fig. 2C). In contrast to mouse adipocyte progenitors, Jak inhibition did not consistently affect general adipogenic gene expression in hMADS and hSVF cells (Fig. 2, A and C). These results suggest an indispensable function of Jak signaling in the beige differentiation of murine and human adipocyte progenitors.

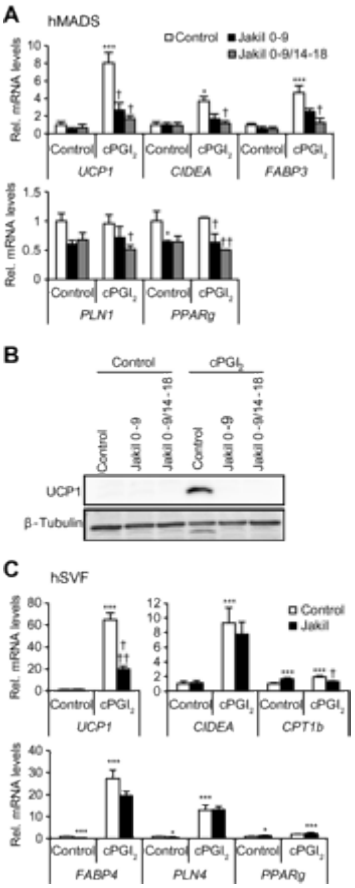

- Download high-res image
- Open in new tab
- Download Powerpoint

Fig. 2 Jak activity is required for human beige adipocyte differentiation.

(**A** and **B**) hMADS cells were subjected to differentiation for 18 days ± $cPGI_2$. Cells were treated with JakiI (0.5 μM) during days 0 to 9 (commitment phase) or 0 to 9 and 14 to 18 before qRT-PCR analysis of thermogenic and adipogenic genes was performed at 18 days (*n* = 3 independent experiments) (A) or Western blotting (representative of two independent experiments) (B). (**C**) hSVF cells from human subcutaneous fat were subjected to differentiation for 18 days ± $cPGI_2$ and ± JakiI. qRT-PCR analysis was performed on thermogenic, mitochondrial, and adipogenic genes (*n* = 3 cultures from one patient). Two-way ANOVA with Bonferroni post hoc comparisons: "*" indicates the difference to control/control, and "†" indicates the difference to $cPGI_2$.

The Jak family of kinases promote progenitor activation and commitment before the induction of Pparg and its targets

The requirement for Jak in thermogenic differentiation apparently contradicts a report demonstrating thermogenic conversion of adipocytes by CP-690550 treatment (*23*). Intriguingly, restriction of JakiI treatment to days 3 to 8 of progenitor differentiation caused significant increases in *Ucp1* and *Cidea* expression, despite inhibitory effects on general adipogenic markers (Fig. 3A). In contrast to this late effect, treatment with JakiI during the first 48 hours of differentiation mirrored the continuous 8-day inhibition and was sufficient to significantly reduce thermogenic gene expression (Fig. 3B). It is noteworthy that the 48-hour Jak inhibition did not affect differentiation markers in the absence of $cPGI_2$. Similarly, Jak inhibition during the commitment phase of hMADS cells (days 0 to 9) (*24*) blunted the induction of thermogenic gene expression (Fig. 2, A and B). These results reveal unexpected opposing roles of Jak in progenitors compared to committed adipocytes, with a dominant requirement of Jak function for thermogenic differentiation during the activation and/or commitment of immature progenitor cells.

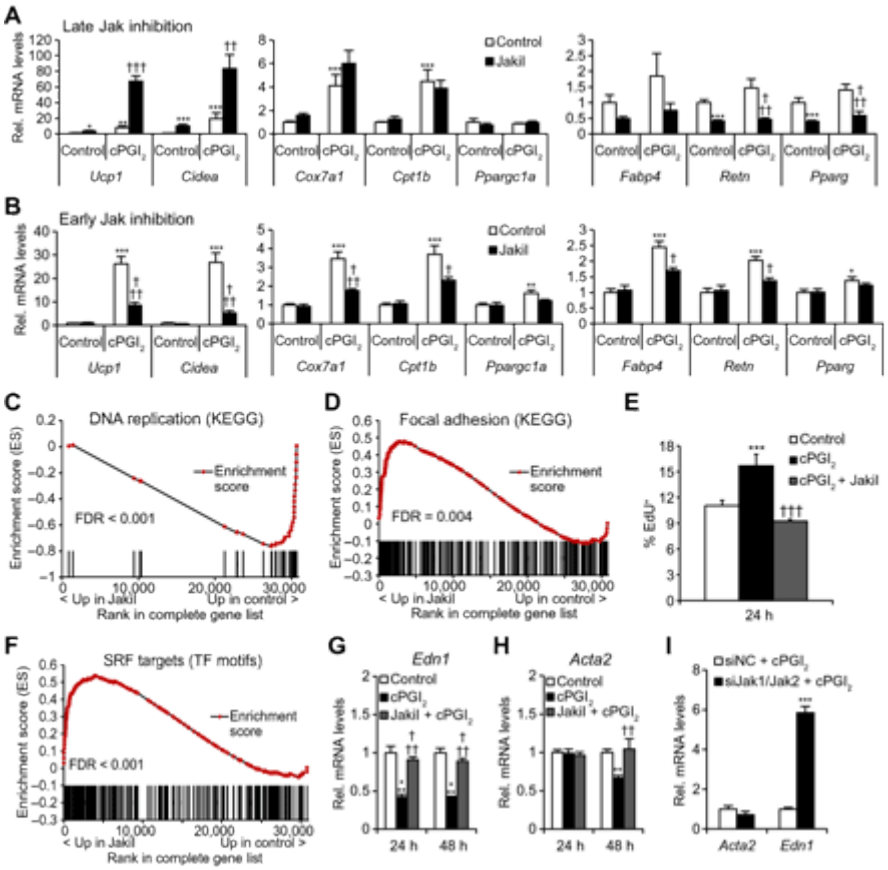

- Download high-res image
- Open in new tab
- Download Powerpoint

Fig. 3 Jak promotes progenitor activation and beige adipogenic commitment.

(**A** and **B**) $Lin^{-}Sca1^{+}$ cells were treated with JakiI (0.2 μM) from day 3 to day 8 of differentiation (A) or for the first 48 hours of differentiation (B) and analyzed at day 8. qRT-PCR analysis was performed on thermogenic, mitochondrial, and adipogenic genes. (**C** to **F**) $Lin^{-}Sca1^{+}$ cells were analyzed at 24 hours of differentiation with $cPGI_2$ in the presence of JakiI (0.2 μM) or vehicle. (C and D) Enrichment plots from GSEA (JakiI compared to control) performed for KEGG (Kyoto Encyclopedia of Genes and Genomes) pathways on microarray expression profiles. FDR, false discovery rate. (E) Cells were labeled with EdU, stained (including propidium iodide), and analyzed by flow cytometry. (F) Enrichment plot from GSEA (JakiI compared to control) with the transcription factor (TF) motif gene set collection. (**G** and **H**) qRT-PCR analysis of $Lin^{-}Sca1^{+}$ cells at 24 or 48 hours of differentiation. (**I**) Cells were transfected with the indicated siRNAs and analyzed at 24 hours of differentiation. (A and C to I) $n = 3$ independent cultures from three or more mice. (B) $n = 5$ independent cultures from three or more mice. "*" indicates the difference to control, and "†" indicates the difference to $cPGI_2$ tested by two-way ANOVA with Bonferroni post hoc comparisons (A and B), one-way ANOVA with Tukey post hoc comparisons (E, G, and H), or Student's *t* test (I).

We then investigated the biological pathways controlled by Jak in immature progenitors. We have previously shown that $cPGI_2$ rapidly induces transient cell cycling and reduced expression of cell adhesion pathways in progenitor cells (*18*). The most significantly suppressed pathway at 24 hours of Jak inhibition was DNA replication, as identified by expression profiling and Gene Set Enrichment Analysis (GSEA) (Fig. 3C) (*25*). Similarly, the $cPGI_2$-mediated reduction in cell adhesion pathway expression was reversed by Jak inhibition (Fig. 3D). Jak inhibition prevented the $cPGI_2$-mediated increase in the fraction of cells in the S phase and reduced incorporation of the nucleotide analog 5-ethynyl-2-deoxyuridine (EdU) during the first 24 hours of differentiation (Fig. 3E and fig. S3, A to C). These results demonstrate that Jak activity promotes the activation of adipocyte progenitors in terms of transient cycling and adhesion, which precede thermogenic differentiation.

The molecular mediators of Jak function in adipocyte progenitors are largely unexplored. The transcription factor Cebpb has been previously implicated as a target of Jak/Stat3 in the regulation of adipogenesis in 3T3-L1 cells (*16*). However, expression of *Cebpb* was not affected by Jak inhibition in primary progenitor cells at 3 or 8 hours (fig. S3D) when Cebpb exerts its critical adipogenic function. Similarly, Jak inhibition did not influence expression of *Zfp423*, which encodes a key adipogenic commitment factor [fig. S3E; (*26*)]. In line with these findings, expression of *Pparg*, a target of both Cebpb and Zfp423 and a master regulator of adipogenesis and browning, or the Pparg targets *Cebpa* and *Fabp4*, were not altered in JakiI-treated cells at 24 hours (fig. S3, F to H). To identify transcription factors regulated by Jak activity at the onset of differentiation and before the expression of *Pparg* increased (fig. S3I), we performed GSEA with target gene sets by transcription factor at 24 hours (*25*). The gene set that was most significantly suppressed by Jak inhibition corresponded to E2F1, which is consistent with the reduction in cell cycling (fig. S3J and Fig. 3E). Intriguingly, the gene set with the most significant increase in expression was serum response factor (Srf) (Fig. 3F), which, in cooperation with its co-regulator Mkl1 (also named MRTFA), inhibits adipogenic commitment and browning in vivo (*27*, *28*). To validate this finding, we

confirmed the increased expression of the Srf/Mkl1 target genes *End1* (which encodes endothelin 1) and *Acta2* (which encodes smooth muscle actin) (*29*, *30*) in progenitors treated with JakiI or Jak1/2 small interfering RNA (siRNA) (Fig. 3, G to I). Together, these results suggest that Jak inhibition affected central pathways of progenitor activation and adipogenic commitment by reducing cell cycling and increasing Srf activity at the very onset of thermogenic differentiation.

The Jak family of kinases inhibit autocrine and paracrine TGFβ signaling to permit commitment and thermogenic differentiation of adipocyte progenitors

We next sought to test the functional relevance of Srf activity downstream of Jak in immature progenitors. To this end, we restricted JakiI treatment to the first 48 hours of differentiation and combined it with CCG-1423, a compound that inhibits Srf and Mkl1 function (*27*, *31*). Inhibition of Srf activity restored the expression of adipogenic and thermogenic genes in JakiI-treated cells to a substantial extent (Fig. 4A), confirming the involvement of Srf in Jak-dependent adipogenic and thermogenic commitment. Srf promotes smooth muscle cell differentiation in response to TGFβ (*32*). We hypothesized that increased TGFβ signaling drove Srf activity upon Jak inhibition and examined the activation of the transcription factor Smad3, which is a separate pathway arm downstream of TGFβ (*33*). The expression of the Smad3 target gene set was significantly increased by Jak inhibition at 24 hours (Fig. 4B). TGFβ stimulation activates Smad3 through phosphorylation at $Ser^{423/425}$ by activin receptor–like kinases (Alk; TGFβ type I receptor) (*33*). Intriguingly, Jak inhibition led to increased Smad3 phosphorylation, which was reversed by the Alk4/5/7 inhibitor SB-431542, thereby confirming the activation of the TGFβ pathway through Jak inhibition [Fig. 4C and fig. S4, A and B; (*34*)]. In contrast, the bone morphogenetic protein (BMP)–dependent phosphorylation of Smad1/5/8 was not altered (Fig. 4D and fig. S4C). To test whether TGFβ receptor inhibition could rescue the Jak inhibition phenotype, we treated progenitors simultaneously with JakiI and SB-431542 during the first 48 hours of differentiation. Strikingly, this treatment restored expression of *Ucp1*, *Cidea*, and other adipogenic and thermogenic genes as well as Ucp1 protein to varying extents at the end of differentiation (Fig. 4, E and F). Thus, these results reveal an unexpected pathway cross-talk, in which Jak activity inhibits TGFβ receptor signaling in immature adipocyte progenitors to restrict smooth muscle gene expression and permit commitment to thermogenic adipogenesis.

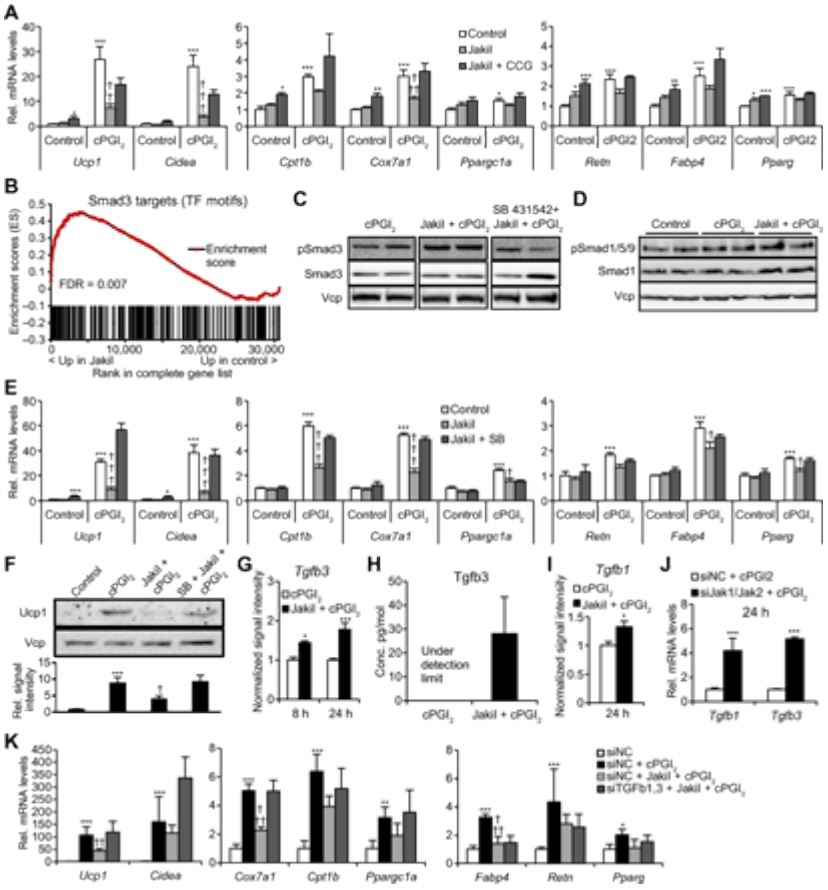

- Download high-res image
- Open in new tab
- Download Powerpoint

Fig. 4 Jak inhibits autocrine and paracrine TGFβ signaling to permit commitment and thermogenic differentiation of adipocyte progenitors.

(**A**) $Lin^{-}Sca1^{+}$ cells were subjected to 8-day differentiation in the presence of $cPGI_2$. Cells were treated with JakiI (0.2 μM) and the Srf inhibitor CCG-1423 (CCG; 10 μM) during the first 48 hours of differentiation and analyzed at 8 days by qRT-PCR for thermogenic, mitochondrial, and adipogenic gene expression. (**B**) GSEA (JakiI compared to control) on $Lin^{-}Sca1^{+}$ cells at 24 hours. (**C** and **D**) $Lin^{-}Sca1^{+}$ cells were differentiated for 48 hours in the presence of the indicated compounds, including the Alk4/5/7 inhibitor SB-431542 (SB; 10 μM). Representative Western blots for pSmad3 ($Ser^{423/425}$) (C) and pSmad1/5/8 ($Ser^{463/465}$) (D) (each lane represents an independent culture, $n = 2$ independent cultures per condition from three or more mice). (**E** and **F**) $Lin^{-}Sca1^{+}$ cells were treated with JakiI (0.2 μM) and SB-431542 during the first 48 hours of differentiation and analyzed at 8 days by qRT-PCR for thermogenic, mitochondrial, and adipogenic gene expression (E) or Western blotting (F) (representative of $n = 3$ independent cultures from three or more mice). (**G** to **I**) $Lin^{-}Sca1^{+}$ cells were differentiated in the presence of $cPGI_2$ and JakiI and analyzed by qRT-PCR (G and I) or by enzyme-linked immunosorbent assay (ELISA) at 48 hours (H). (**J** and **K**) $Lin^{-}Sca1^{+}$ cells were transfected with the indicated siRNA and subjected to differentiation. qRT-PCR analysis was performed at 24 hours (J) and 8 days for thermogenic and mitochondrial genes (K). "*" indicates the difference to $cPGI_2$ (A, E, G, I, and J) or to siNC (K), and "†" indicates the difference to JakiI + $cPGI_2$ (A and E) or to siNC + $cPGI_2$ (K), tested by two-way (A, E,

and K) ANOVA or *t* test (G, I, and J); (A and B and E to K) *n* = 3 to 4 independent cultures from three or more mice.

Because Jak-TGFβ cross-talk was detectable over at least 1 to 2 days, we suspected a transcriptional mechanism and mined the expression profiles of JakiI-treated immature progenitors for candidate target genes. The expression of *Tgfb3* was significantly induced by Jak inhibition as early as 8 hours of treatment, which persisted at 24 hours and resulted in the detection of secreted Tgfb3 in the supernatant (Fig. 4, G and H). In addition, expression of *Tgfb1* was moderately but significantly increased by JakiI at 24 hours (Fig. 4I). Consistently, *Jak1/2* double knockdown robustly increased *Tgfb3* and *Tgfb1* expression (Fig. 4J). To test whether these changes were functionally relevant to the differentiation of progenitors, we silenced *Tgfb3* and *Tgfb1* by siRNA. Although single knockdown was insufficient to rescue the Jak inhibition phenotype, knockdown of both *Tgfb1* and *Tgfb3* largely restored thermogenic gene expression (Fig. 4K and fig. S4, D to G).

Stat3 mediates Jak-TGFβ cross-talk and is required for progenitor differentiation in vivo

The strong acute suppression of *Socs3* expression by JakiI treatment suggested the involvement of the transcription factor Stat3 as a direct substrate of Jak activity, which was confirmed by assaying Stat3-Tyr^{705} phosphorylation in progenitors (figs. S1I and S5, A and B). siRNA knockdown of *Stat3* in immature progenitors concomitantly reduced *Socs3* expression and increased *Edn1* and *Acta2* expression, confirming the notion that Stat3 could mediate the inhibition of TGFβ-Srf target gene expression (Fig. 5A and fig. S5, C to E). Consistently, we found that *Tgfb3* expression was robustly elevated upon *Stat3* knockdown at 8 and 24 hours of differentiation (Fig. 5B). Next, we used the adipogenic C3H10T1/2 mesenchymal progenitor cell line to obtain sufficiently high cell yields for chromatin immunoprecipitation (ChIP). We observed marked enrichment of the *Tgfb3* proximal promoter but not of the unrelated sequences of *Tbp* exon 3 upon ChIP for phosphorylated Stat3-Tyr^{705}, suggesting a direct involvement of phosphorylated Stat3 in the regulation of *Tgfb3* transcription (Fig. 5C). In support of the involvement of activated Stat3 in the repression of the *Tgfb3* gene, using transient reporter assays, we found that the activity of the *Tgfb3* promoter was reduced by expression of wild-type Stat3 or the constitutively active Stat3^{Y640F} mutant but increased by expression of the dominant-negative Stat3^{Y705F} mutant [Fig. 5D; (*35*, *36*)]. These results suggest that Jak/Stat3 interfere with autocrine and paracrine TGFβ signaling by inhibiting the expression of the *Tgfb3* ligand-encoding gene at the promoter level. Finally, we tested the functional importance of *Stat3* for progenitor differentiation. *Stat3* knockdown caused a reduction in adipogenic and thermogenic gene expression to a degree comparable to prolonged JakiI treatment (Fig. 5E). To validate this finding under in vivo conditions, we transplanted *Stat3*$^{F/F}$ progenitors after transfection with Cre mRNA subcutaneously into *Stat3*$^{+/+}$ mice and examined the formation of adipocytes after 4 weeks (Fig. 5F and fig. S5, F to H). *Stat3* deficiency in donor cells resulted in Matrigel plugs with a comparable number of nuclei but a markedly reduced frequency of adipocytes compared to control *Stat3*$^{F/F}$ plugs, arguing for a critical function of Stat3 in the commitment of immature progenitors to adipogenesis.

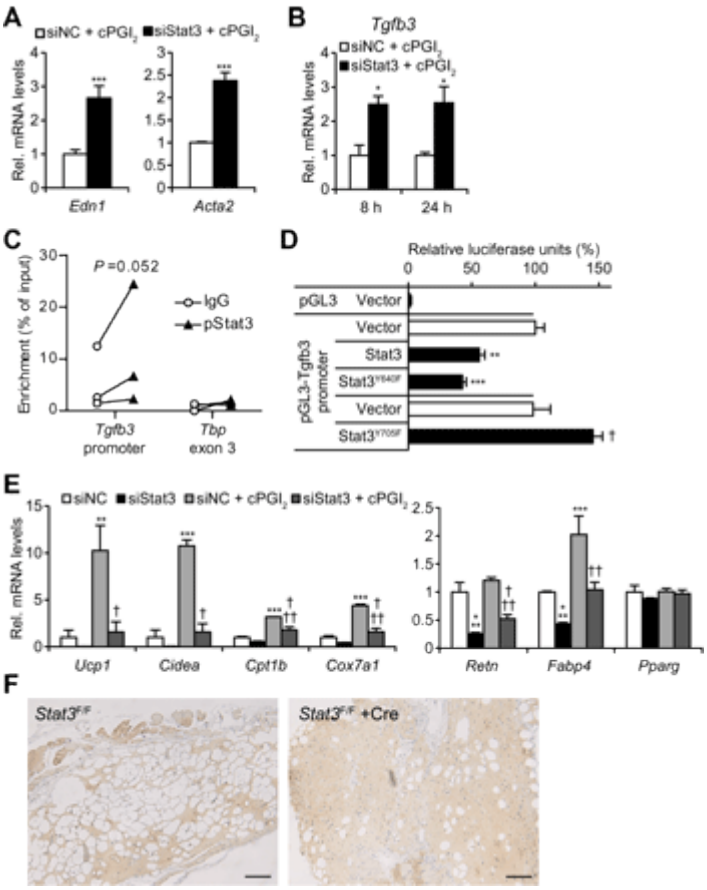

- Download high-res image
- Open in new tab
- Download Powerpoint

Fig. 5 Stat3 inhibits TGFβ signaling in progenitors and is required for progenitor differentiation.

(**A** and **B**) $Lin^{-}Sca1^{+}$ cells were transfected with the indicated siRNAs, subjected to differentiation, and analyzed by qRT-PCR at 48 hours (A) or 8 and 24 hours (B). (**C**) Quantitative PCR (qPCR) for the indicated genomic locations from ChIP analysis on mesenchymal C3H10T1/2 progenitor cells with phospho-Stat3 (Tyr^{705}) and immunoglobulin G (IgG) antibodies. $n = 3$ independent experiments; *t* test, *P* value indicates the difference to IgG. (**D**) Arbitrary luciferase units (percentage relative to vector) from reporter assay in C3H10T1/2 cells cotransfected with the Tgfb3 promoter-reporter and the indicated Stat3-expressing plasmids. $n = 3$ independent experiments. "*" and "†" indicate difference to the corresponding vector controls by one-way ANOVA with Tukey posttest and *t* test, respectively. (**E**) $Lin^{-}Sca1^{+}$ cells were transfected with the indicated siRNAs, subjected to differentiation, and analyzed by qRT-PCR for thermogenic and mitochondrial gene expression at day 8. (**F**) $Lin^{-}Sca1^{+}$ cells from $Stat3^{F/F}$ mice were transfected with Cre recombinase or control mRNA and injected subcutaneously in Matrigel into $Stat3^{wt}$;*UBC-GFP* mice. Sections of Matrigel plugs at 4 weeks after injection were stained with hematoxylin (representative images from $n = 3$ mice for each condition; scale bars, 20 μm). *t* test (A and B) ($n = 4$ independent cultures from three or more mice) and two-way ANOVA (E) with post hoc comparisons ($n = 3$ independent cultures from three or more mice). "*" indicates the difference to siNC + $cPGI_2$ (A and B) or to siNC (E), and "†" indicates the difference to siNC + $cPGI_2$ (E).

Jak/Stat3 activation and Tgfb3 are downstream of β-adrenergic lipolytic activation in the adipose tissue microenvironment

We next sought to determine whether the Jak-Stat3-TGFβ signaling axis is activated in an in vivo model of progenitor differentiation. To this end, we used the β3-adrenoreceptor agonist CL-316243, which induces progenitor-mediated recruitment of beige and white adipocytes as shown by fate mapping (*2*, *4*, *11*, *37*). We focused on the first hours of stimulation as we did in the ex vivo model. Injection of CL-316243 led to increased Stat3-Tyr^{705} phosphorylation in adipose tissue within 6 hours, which was mainly detectable in stromal cells (Fig. 6, A to C). This was accompanied by acute increase in *Socs3* expression, which was of transient nature because it was reversed after 7 days of CL-316243 infusion (Fig. 6, D and E). These effects were associated with decreased expression of *Tgfb1* and particularly *Tgfb3* mRNA and protein by 8 hours (Fig. 6, F to H). Acute triglyceride lipolysis induces transient inflammation in adipose tissue (*38*–*41*). Therefore, we examined the effect of adipocyte-specific genetic inactivation of the adipose triglyceride lipase (ATGL) on Jak-Stat3-Tgfb3 regulation. ATGL (which is encoded by *Pnpla2*) deficiency prevented the acute CL-316243–mediated lipolytic response, Stat3 phosphorylation, the increase in *Socs3* expression, and the decrease in *Tgfb3* expression (Fig. 6, I to L, and fig. S6A), suggesting that lipolysis is the initial trigger of this pathway downstream of β-adrenergic stimulation.

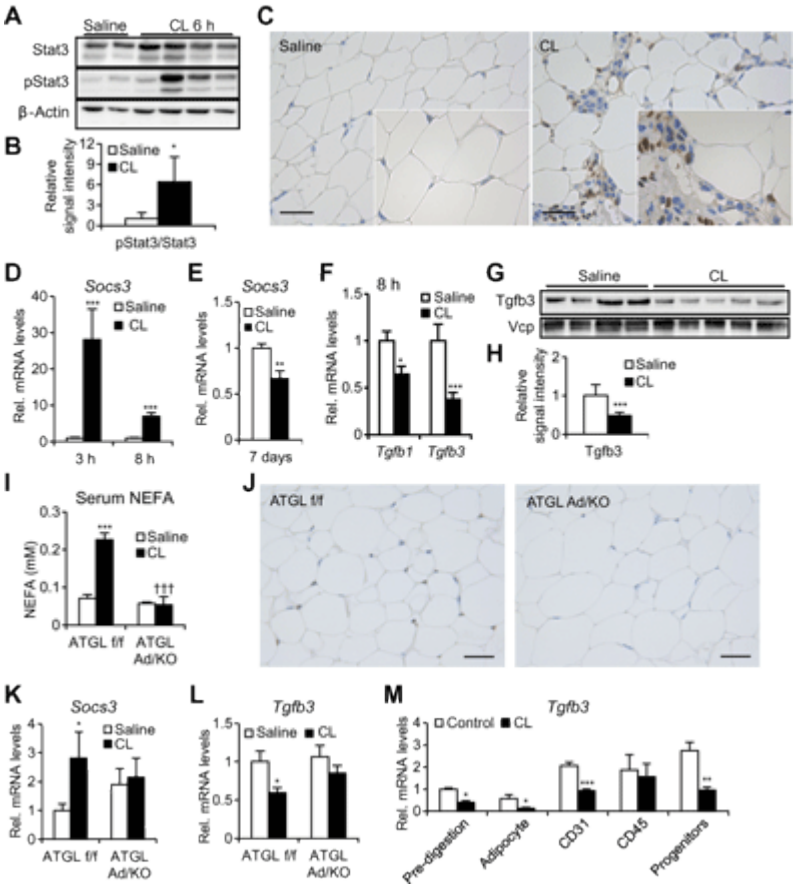

- Download high-res image
- Open in new tab
- Download Powerpoint

Fig. 6 Lipolysis-dependent Jak/Stat3 activation and Tgfb3 regulation at the onset of β-adrenergic adipose tissue remodeling.

Adipose tissue analysis from mice treated with a single injection (**A** to **D** and **F** to **M**) or continuous infusion (**E**) of the β3-adrenergic agonist CL-316243 (CL) or saline. (A) Representative Western blot of pStat3 (Tyr^{705}) 6 hours after injection. (B) Quantitative image analysis of (A). (C) Representative immunohistochemistry of phospho-Stat3 (Tyr^{705}) 6 hours after injection. (A to C) *n* = 4 (saline)/7 (CL-316243) mice. (D to F) qRT-PCR analysis (*n* = 5 mice for each condition and time point). (G) Representative Western blot at 6 hours. (H) Quantitative analysis of (G). *n* = 4 (saline)/5 (CL-316243) mice. (I to L) Mice were analyzed 3 hours after injection with CL-316243 or saline (*n* = 12 mice for each condition). (I) Serum nonesterified fatty acids (NEFAs). (J) Representative immunohistochemistry of phospho-Stat3 (Tyr^{705}) on sections from CL-316243–treated mice. (K and L) qRT-PCR. (M) The indicated cell populations were sorted by fluorescence-activated cell sorting (FACS) 16 hours after injection with CL-316243 or saline and analyzed by qRT-PCR (*n* = 3 sorted samples from six mice for each condition). "Progenitors" = $Lin^{-}CD29^{+}CD34^{+}Sca1^{+}$. *t* test (A to H and M) and two-way ANOVA (I, K, and L) with Bonferroni post hoc comparisons: "*" indicates the difference to saline (A to M). Scale bars, 50 μm (C and I).

To test whether Jak-Stat3-Tgfb3 was induced in progenitor cells, we sorted $Lin^{-}CD29^{+}CD34^{+}Sca1^{+}$ progenitors, mature adipocytes, endothelial ($CD31^{+}$) cells, and leukocytes ($CD45^{+}$) from CL-316243– and saline-treated mice. The cell isolation procedure acutely increased *Socs3* expression, thereby precluding the analysis of Jak/Stat3 activation in sorted cells (fig. S6B). Nevertheless, expression of *Socs3* was highest in progenitor cells, indicating their high sensitivity for this pathway. The expression of *Tgfb3* was not affected by tissue digestion and was highest in progenitor cells compared to the other cell types (Fig. 6M). Intriguingly, CL-316243 treatment resulted in a significant acute decrease in *Tgfb3* expression in all cell types except leukocytes (Fig. 6M). Because progenitors showed the highest *Tgfb3* expression that was potently suppressed by CL-316243, we expect that progenitors substantially contribute to the altered Tgfb3 protein levels in the microenvironment.

Transient IL-6 family activation mediates Jak/Stat3-Tgfb3 signaling in progenitors and adipose tissue

IL-6 cytokine family members are potent inducers of the Jak/Stat3 pathway, and IL-6 is induced by β-adrenergic stimulation (*40*, *42*–*44*). We confirmed the potent acute increase in *Il6* expression upon CL-316243 treatment, which was transient in nature (Fig. 7A). In addition, we detected a similar expression pattern for the mRNA encoding IL-11, which has similar signaling activities to IL-6 (Fig. 7B). Comparing the expression of the IL-6 family receptor-encoding genes in progenitors revealed *Il11ra1* as the highest expressed (Fig. 7C). In accordance, recombinant IL-11 had about 10-fold higher potency compared to IL-6 in inducing *Socs3* in progenitors ex vivo (Fig. 7, D and E). Furthermore, progenitors responded to IL-11 by reducing *Tgfb3* expression even at 1 ng/ml, whereas only a modest trend was observed for IL-6 at 100 ng/ml (Fig. 7, F and G). Acute treatment of mice with IL-11 robustly induced Stat3-Tyr^{705} phosphorylation and *Socs3* in adipose tissue, which was accompanied by a twofold reduction of *Tgfb3* but not *Tgfb1* (Fig. 7, H to J, and fig. S7A). These results unexpectedly demonstrated that progenitors were highly sensitive to IL-11 and that this cytokine could directly mediate the decreased *Tgfb3* expression in progenitors and in vivo. IL-11 inhibits adipogenesis in cell lines, and consistently, chronic stimulation of differentiating progenitors markedly reduced thermogenic and adipogenic gene expression in our system [fig. S7B; (*45*)]. In contrast, we observed that transient stimulation of immature progenitors with IL-11 increased their potential for thermogenic adipocyte differentiation (Fig. 7K). Together, these results suggest that the transient wave of IL-6 family cytokines and

particularly IL-11 can activate the Jak/Stat3-Tgfb3 axis, thereby promoting activation and commitment of progenitors in the context of β-adrenergic adipose tissue remodeling (Fig. 8).

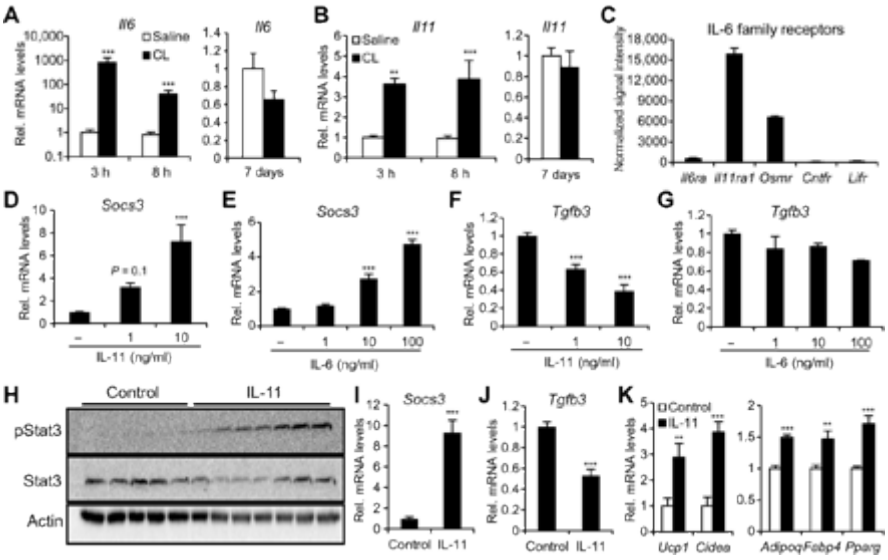

- Download high-res image
- Open in new tab
- Download Powerpoint

Fig. 7 IL-11 triggers the Jak/Stat3-Tgfb3 axis in progenitors and in adipose tissue.

(**A** and **B**) qRT-PCR analysis from mice treated with a single injection or continuous infusion of CL-316243 or saline (n = 5 mice for each treatment). (**C**) mRNA expression profiling from Lin^-Sca1^+ cells (n = 3 independent cultures from three or more mice). (**D** to **G**) Lin^-Sca1^+ cells were treated with the indicated cytokines and analyzed by qRT-PCR at 24 hours (n = 3 independent cultures from three or more mice). (**H** to **J**) Mice were injected with IL-11 (500 μg/kg) or vehicle, and adipose tissue was analyzed by Western blotting (H) and qRT-PCR (I and J) at 3 hours after injection. n = 5 (control)/7 (IL-11) mice. (**K**) Lin^-Sca1^+ cells were pretreated with IL-11 [20 ng/ml in 1% bovine serum albumin (BSA)] for 6 hours, subjected to differentiation for 8 days, and analyzed by qRT-PCR (n = 4 independent cultures from three or more mice). t test (A, B, and I to K) and one-way ANOVA with Tukey posttests (D to G). "*" indicates the difference to saline (A and B) or to control (D to K).

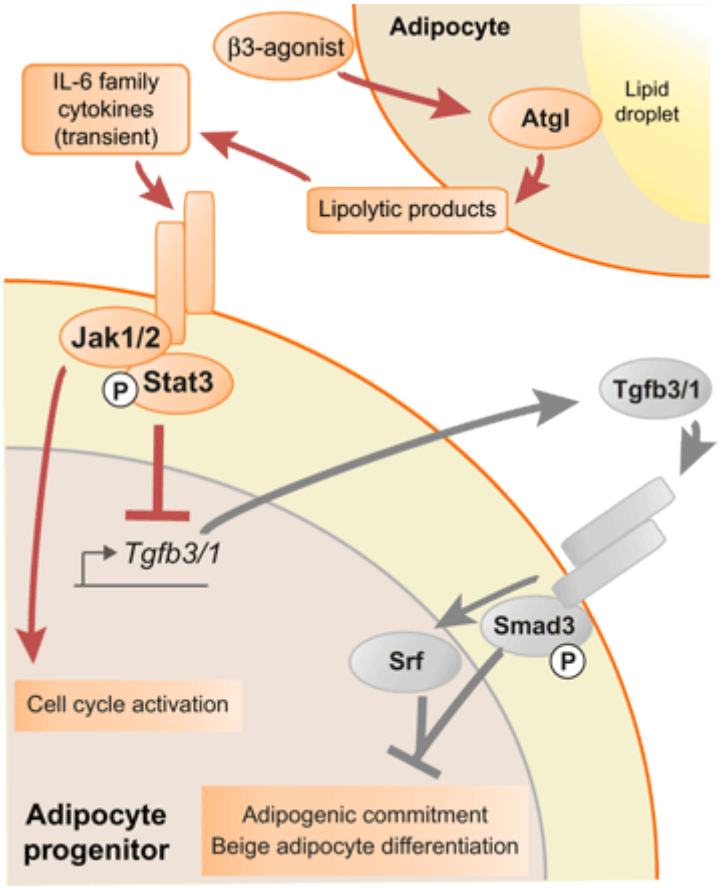

- Download high-res image
- Open in new tab
- Download Powerpoint

Fig. 8 Jak/Stat3 links transient lipolytic or inflammatory stress to adipocyte progenitor activation through local regulation of TGFβ signaling.

Upon lipolytic stimulation, IL-6 family cytokines (IL-11 and IL-6) are transiently elevated and activate Jak/Stat3 signaling in adipocyte progenitors. Jak activation accelerates the cell cycle, an activation step for differentiation, and also alleviates the constitutive inhibitory effects of TGFβ to promote adipogenic commitment and thermogenic beige adipocyte differentiation by repressing autocrine and paracrine Tgfb3/1 signaling through Stat3. Chronic stimulation of the pathway results in repression of adipogenic and thermogenic differentiation.

DISCUSSION

The links between immune and inflammatory mediators and adipocyte progenitor regulation during adipose tissue remodeling are poorly understood. Here, we showed that Jak/Stat3 signaling controlled local TGFβ action in response to lipolysis-dependent transient inflammation and thereby adipogenic progenitor commitment and thermogenic differentiation (Fig. 8). The severe Jak/Stat3 mouse knockout phenotypes, along with their cooperative functions and the lack of genetic tools specifically targeting adipocyte progenitors, has so far limited functional analysis in this cell type. Derecka *et al*. (*46*) have shown a requirement for Tyk2 in classical brown adipocyte differentiation. However, we observed that in white fat progenitors, Jak1/2, but not Tyk2, seem to be crucial for Stat3 activation (fig. S1H). In

agreement with this finding, the Jak1/2/3-selective inhibitor CP-690550 or Jak1/2 double knockdown was sufficient for the strong inhibition of thermogenic gene expression (Fig. 1G and fig. S1D). The Jak family of kinases have been implicated in the differentiation of white preadipocyte cell lines, particularly in the induction of the master regulators *Cebpb*/*Cebpd* and *Pparg* (*15*, *16*, *47*). Beyond this, only limited information is available on the downstream target genes in this context (*14*). The regulation of *Cebpb* or *Pparg* expression by Jak during differentiation induction could not be confirmed in primary progenitors (fig. S3, D and F). Moreover, Jak inhibition affected the TGFβ-Srf/Smad3 pathway and its targets before any changes in *Pparg* expression or activity could be detected. Thus, we propose that interference with TGFβ signaling is a primary target of Jak in defined adipocyte progenitors. Continuous Jak/Stat3 inhibition compromised general adipocyte differentiation (Figs. 1 and 5 and fig. S1), which is consistent with previous studies and the ability of TGFβ, Srf, and Bmp7 to control both general and thermogenic adipogenesis (*27*, *28*, *48*, *49*). However, restriction of Jak inhibition to the commitment phase only affected $cPGI_2$-stimulated beige adipocyte differentiation (Figs. 3B and 4, A and E). In addition, the effects of Jak/Stat3 inhibition were generally more pronounced under $cPGI_2$ compared to control and for thermogenic markers compared to white differentiation markers. Together, our findings suggest that although Jak/Stat3 appear to influence later stages of white adipogenesis, Jak-Stat3-TGFβ activity is critical for beige adipogenesis during the activation and commitment of murine and human progenitors.

Although the TGFβ-Srf/Smad3 pathway is a critical inhibitor of browning in vivo, Bmp7 is the only known physiological factor that counteracts this pathway in adipose tissue (*27*, *49*). Our findings uncover the Jak/Stat3-Tgfb3 axis as a Bmp7-independent mechanism that controlled TGFβ activity in progenitors. We demonstrated that adipocyte progenitors were a main source of Tgfb3 in the adipose tissue microenvironment and that autocrine and paracrine Tgfb3 and Tgfb1 signaling restricted adipogenic commitment of progenitors (Figs. 4K and 6M). Jak activity inhibited expression of *Tgfb3* and *Tgfb1* through Stat3 and counteracted TGFβ-Srf/Smad3 activation. It is tempting to speculate that chronic dysregulation of Tgfb3 and Tgfb1 in progenitor and stromal cells may promote fibrosis and inhibit adipogenesis and mitochondrial oxidative metabolism, contributing to adipose tissue dysfunction and metabolic disease (*49*, *50*).

The Jak/Stat3-Tgfb3 cross-talk was triggered by IL-6 family cytokines and particularly IL-11 in isolated progenitors and in vivo (Fig. 7). The observed wave of IL-6 family cytokine production upon CL-316243 administration confirms previous reports linking lipolysis to transient inflammation (*38*–*40*, *42*, *44*). Stat3 activation and decreased *Tgfb3* expression depended on ATGL-mediated lipolysis in our model (Fig. 6). The involvement of lipolytic products as signaling mediators in the induction of thermogenic gene expression is supported by previous studies interfering with lipase function (*39*, *51*–*53*). Given its promiscuity, it is likely that the Jak/Stat pathway may be activated by other stimuli that promote browning and adipogenesis, such as growth factors or type 2 cytokines (*10*, *13*, *14*). Nevertheless, we identify an upstream activator of Jak/Stat linking to a progenitor function in a physiological context. We propose that the signaling cascade presented here may be relevant for stress-induced beige and possibly white adipogenesis as observed during β-adrenergic tissue remodeling (*2*, *4*, *9*). However, the markedly reduced adipogenic commitment upon transplantation of *Stat3*-deficient progenitors supports a broader requirement of Jak/Stat3 in adipogenesis (Fig. 5).

The proposed role of IL-6 family cytokines in adipocyte progenitor activation/commitment appears paradoxical. Prolonged stimulation of differentiating progenitors with IL-11 inhibited

adipogenesis (fig. S7B), which agrees with previous findings in cell lines and with the inhibition of browning by chronic oncostatin M administration (*45*, *54*). Surprisingly, a pulse of IL-11 stimulation in immature progenitors increased their adipogenic potential in culture (Fig. 7). This was associated with reduced *Tgfb3* expression, which was recapitulated by a single bout of IL-11 in vivo, mimicking the transient induction of IL-11 by CL-316243. Moisan *et al*. (*23*) reported that Jak inhibition in adipocytes increased thermogenic expression, which we confirmed in postcommitment progenitors (Fig. 3A). The differential outcome of Jak signaling in immature compared to committed cells requires further investigation. Nonetheless, these findings collectively suggest that the transient activation of Jak/Stat3 is important for progenitor activation and thereby the initiation of tissue remodeling, whereas chronic activation results in repression of adipogenic/thermogenic function. Our model reinforces the idea that transient inflammation promotes the induction of adaptive adipose tissue remodeling, which should be taken into consideration in therapeutic approaches targeting inflammatory pathways in adipose tissue.

MATERIALS AND METHODS

Mice

Animal handling and experimentation were approved by local authorities (Regierungspräsidium Karlsruhe) to ascertain the fulfillment of the European Union directives and the German Animal Welfare Act (Tierschutzgesetz) or by the University of Pittsburgh Institutional Animal Care and Use Committee. Seven- to 12-week-old female mice were housed at 22°C with free access to chow diet (Kliba Nafag #3437, Provimi Kliba) ad libitum on a 12-hour light-dark cycle. NMRI mice (Charles River WIGA GmbH) were used unless otherwise indicated. To generate adipocyte-specific ATGL knockout mice (ATGL-AdKO), mice carrying a loxP-modified *Pnpla2* (Atgl) allele (B6N.129SPnpla2^{tmEek}, shortened to ATGL-f/f here) (*41*) were crossed with mice harboring Cre recombinase under the control of the adiponectin promoter [B6N.FVB.Tg(Adipoq-Cre)^{1evr}/J] (*55*). Stat3$^{F/F}$ (B6.Cg-Stat3^{tm2Aki}) and UBC-GFP [C57BL/6-Tg(UBC-GFP)$^{30Scha/J}$] mice were obtained from The Jackson Laboratory. For in vivo β-adrenergic stimulation, mice were either intraperitoneally injected with CL-316243 (1 mg/kg; R&D Systems GmbH) or equivalent volume of saline (acute treatments) or subcutaneously implanted with Alzet minipumps (DURECT Corporation) delivering saline or CL-316243 (1 mg/kg per day). The animals were sacrificed at the indicated time points by cervical dislocation, and perigonadal fat was dissected and processed. NEFAs were measured in serum samples using the NEFA-HR (*2*) kit (Wako Chemicals) according to the manufacturer's instructions.

SVF preparation from human and mouse adipose tissue

Human abdominal subcutaneous fat biopsies were obtained during bariatric surgery at the Department of Surgery, University Hospital Heidelberg, based on approval by the Institutional Review Board of the Medical Faculty of the University of Heidelberg in accordance with the Declaration of Helsinki and its later amendments. Informed consent was obtained individually from each patient. Murine or human biopsies were mechanically minced with scissors and digested in Hanks' balanced salt solution (Sigma-Aldrich) supplied by purified collagenase (0.1 Wünsch unit/ml; LS005273, Worthington Biochemical), neutral protease (2.4 U/ml; LS02104, Worthington Biochemical), 4 mM calcium chloride, and deoxyribonuclease I (0.05 mg/ml; 1284932001, Roche Diagnostics) for 50 min at 37°C, agitating at 70 rpm in a shaker. The digested tissue was strained through a 300-μm nylon

mesh (4-1411, Neolab). SVF was pelleted by centrifugation at 145*g* for 10 min at 20°C and consequently washed and centrifuged at 300*g* for 5 min at 20°C.

Progenitor isolation by MACS

Adipose progenitors were isolated by magnetic-activated cell sorting (MACS) approach, as previously described (*17*, *18*). Briefly, the SVF obtained from posterior subcutaneous (inguinal) fat adipose tissue was suspended in BSA buffer [Dulbecco's phosphate-buffered saline (D-PBS), 0.5% BSA, 1 mM EDTA] and incubated with Fc Block (anti-CD16/32, eBioscience) for 10 min on ice. Erythrocytes, endothelial cells, and hematopoietic cells were labeled with biotin-conjugated Ter119 (TER-119), CD31 (390), and CD45 (30-F11) antibodies (eBioscience), 30 min on ice, for later depletion. The labeled cells were washed and incubated with Streptavidin MicroBeads (130-048-102, Miltenyi Biotec) and depleted using an OctoMACS Separator according to the manufacturer's instructions. The collected Lin^- cells were incubated with Sca1 MicroBeads (130-106-641, Miltenyi Biotec) and isolated by magnetic separation according to the manufacturer's instructions.

Isolation of adipose tissue cell populations by FACS

Sorting of adipose tissue cell populations was performed as previously described (*18*). Briefly, adipocytes and SVF were separated by centrifugation of digested and strained adipose tissue. Floating adipocytes were lysed in QIAzol for further analysis, and the SVF was suspended in BSA buffer and incubated with Fc Block for 10 min on ice. To deplete the erythrocytes, the cells were incubated with Anti-Ter-119 MicroBeads (130-049-901, Miltenyi Biotec) for 15 min on ice and applied to an OctoMACS Separator according to the manufacturer's instructions. The collected flow-through was stained for specific cell populations with CD45–fluorescein isothiocyanate (30-F11, eBioscience), CD31–eFluor 450 (390, eBioscience), CD29–peridinin chlorophyll protein complex–eFluor 710 (HMb1-1, eBioscience), CD34–Alexa Fluor 647 (RAM34, BD Biosciences), and Sca-1–Alexa Fluor 700 (D7, eBioscience) for 30 min on ice. Cells were washed, and sorting was performed on a BD FACSAria (BD Biosciences) by using unstained and FMO-stained as negative controls. Compensation was performed by single antibody-stained cells. Sorted cells were pelleted by centrifugation and lysed in QIAzol for further analysis.

Primary cell transplantation

Primary MACS-isolated Lin^-Sca1^+ cells from *Stat3*$^{F/F}$ mice were cultured as described above and transiently transfected with StemMACS Cre recombinase or eGFP mRNA (Miltenyi Biotec) at 500 ng/ml using Lipofectamine RNAiMAX (2 μl/ml). Twenty-four hours after transfection, cells were trypsinized and resuspended (10×10^5/ml) in Matrigel (BD). UBC-GFP mice were substernally injected with 100-μl cell suspension. Mice were euthanized 4 weeks later, and the plugs were dissected.

Primary cell culture and adipogenic differentiation

Human fat–derived SVF or mouse MACS-isolated Lin^-Sca1^+ progenitors [from posterior subcutaneous (inguinal) fat] were plated out on BioCoat Laminin-coated plates (BD Biosciences) and maintained in growth medium [Dulbecco's modified Eagle's medium (DMEM), 10% fetal calf serum (FCS), 1% penicillin/streptomycin (Life Technologies), murine or human basic fibroblast growth factor (10 ng/ml; R&D Systems)], without passaging

for mouse cells, and up to three passages for human cells. Adipogenic differentiation was induced at confluence with induction medium [DMEM, 10% FCS, 1% penicillin/streptomycin, insulin (1 μg/ml), 500 nM dexamethasone, 3 nM triiodothyronine (T3); Sigma-Aldrich] for 2 days. To reach full differentiation, cells were maintained in induction medium with 5% FCS and without dexamethasone for 6 or 17 days for mouse or human cells, respectively. Differentiation was performed in the presence of 1 μM $cPGI_2$ (BIOZOL) unless otherwise indicated. JakiI (Merck Millipore), CP-690550 (R&D Systems GmbH), CCG-1423 (Biomol), SB-431542 (Cayman Chemical), or recombinant murine IL-11 (PeproTech) was added at the indicated concentrations according to the experimental design, or the corresponding concentration of ethanol and dimethyl sulfoxide was added as control. Media ± $cPGI_2$ and inhibitors were replaced freshly every day.

C3H10T1/2 and hMADS cell culture and adipogenic differentiation

C3H10T1/2 cells (American Type Culture Collection) were cultured in DMEM, 10% FCS, and 1% penicillin/streptomycin. The establishment, characterization, and culture protocols of hMADS cells have been described previously (*24*, *56*, *57*). In the experiments reported here, hMADS-3 cells were used, originally isolated from the prepubic fat pad of a 4-month-old male patient. Cells were used between passages 14 and 20. Briefly, confluent cells were submitted to differentiation medium [DMEM/Ham's F12 media containing transferrin (10 μg/ml), 10 nM insulin, and 0.2 nM triiodothyronine] supplemented with 1 μM dexamethasone and 500 μM 3-isobutyl-1-methylxanthine in the presence of $cPGI_2$ (1 μM) and/or JakiI (0.5 μM). Two days later, the medium was changed, dexamethasone and isobutyl-methylxanthine were omitted, and 100 nM rosiglitazone was included up to day 9 with $cPGI_2$ and JakI as indicated. After 5 days in the absence of rosiglitazone and/or $cPGI_2$, white adipocytes were treated with $cPGI_2$ and/or JakiI between days 14 and 18. Medium was changed every day. At day 18, cells were harvested for mRNA or protein expression analysis.

siRNA transfection

MACS-isolated Lin^-Sca1^+ mouse progenitors were transfected by siRNAs specific for *Stat3* (pooled Stat3MSS209601, Stat3MSS277377, and Stat3MSS277378; Life Technologies), *Tgfb1* (Tgfb1MSS211649-651, Life Technologies), *Tgfb3* (Tgfb3MSS211655-657, Life Technologies), *Jak1* (SI01079295 and SI01079302, Qiagen), *Jak2* (SI01079323 and SI01079337, Qiagen), *Jak3* (SI01079351 and SI01079365, Qiagen), *Tyk2* (SI01459479 and SI01459486), and negative control (12935-300, Life Technologies; 1027280, Qiagen) using Lipofectamine RNAiMAX (Life technologies) according to the manufacturer's instructions. Briefly, siRNAs and RNAiMAX (2 μl/ml) were diluted in Opti-MEM (Life Technologies). The diluted siRNAs and reagent were mixed and incubated for 5 min at room temperature. The mixture was added up by DMEM + 10% FCS and transferred to the cells at 10 nM (Life Technologies) or 20 nM (Qiagen) final siRNA concentration. The cells were maintained in transfection medium for 24 hours.

Luciferase promoter-reporter assay

The region −1263 to +157 base pairs (bp) (relative to the transcriptional start site) of the *Tgfb3* locus was amplified by PCR on C57BL/6 genomic DNA with 5′-TTATGAGCTCCCAGCTCCGGAGGAATGG-3′ (forward) and 5′-GCATCTCGAGTCCGCAAAGCTTTTCCCG-3′ (reverse) primers and inserted as a Sac I/Xho I fragment into pGL3 basic (Promega) to yield pGL3-Tgfb3. pGL3 basic (pGL3)

served as negative control. pCEP4-mStat3 and pCEP4-Stat3-Y640F (*35*), which were provided by C. Garbers (Christian-Albrechts-University, Kiel, Germany), were used for expression of wild-type Stat3 and mutant $Stat3^{Y640F}$, with pCEP4 as negative control (Vector). pRc/CMV-Stat3-Y705F (*36*), a gift from J. Darnell (Addgene plasmid #8709), was used for expression of the $Stat5^{Y705F}$ mutant with pRc/CMV as negative control (Vector). pRL-TATA-Renilla was a gift from F. Rösl [Deutsches Krebsforschungszentrum (DKFZ), Heidelberg]. pGL3-Tgfb3 was transiently cotransfected with the indicated Stat3 expression vector and pRL-TATA-Renilla into C3H10T1/2 cells using polyethylenimine HCl (linear; molecular weight, 40,000; Polysciences). Twenty-four hours after transfection, cells were treated with differentiation induction medium for 2 days [DMEM, 10% FCS, 250 nM dexamethasone, 500 μM 3-isobutyl-1-methylxanthine (Sigma-Aldrich), recombinant human insulin (1 μg/ml), and 3 nM T3]. Cell extracts were prepared and analyzed with the Dual-Luciferase Reporter Assay System (Promega) according to the manufacturer's instructions. Firefly luciferase values (arbitrary light units) were background-corrected and normalized using the Renilla luciferase values.

Oil Red O staining

To assay adipogenic efficiency, cells were stained with Oil Red O (Sigma-Aldrich) at the end of differentiation. Cells were fixed in 10% formalin for 1 hour, washed with water, and incubated in 60% isopropanol for 5 min. Isopropanol was discarded and replaced with Oil Red O (2.1 mg/ml in 60% isopropanol) for 20 min. Oil Red O was discarded, and cells were washed with water. Cultures were imaged with an Axio Observer Z1 (Carl Zeiss) microscope using a 10×/0.3 PlnN Ph1 objective and ZEN software (Zeiss).

Cellular respiration assay (Seahorse)

Cellular respiration was analyzed using the XF Cell Mito Stress Test Kit (Agilent) according to the manufacturer's instructions. Briefly, MACS-isolated progenitors were cultured on a XF96 PS microplate at 2000 cells per well. The adipogenic differentiation protocol was applied in the presence of 5 μM $cPGI_2$ and 1 μM JakiI. A calibration plate was prepared by incubating seahorse calibrant medium overnight at 37°C in a CO_2-free incubator. On the day of measurement (day 8 of differentiation), plates were subjected to XF96 extracellular flux analyzer. After three measurements of basal respiration, oligomycin (4 μM), NE (0.5 μM), carbonyl cyanide *p*-trifluoromethoxyphenylhydrazone (FCCP) (2 μM), and rotenone/antimycin A (1 μM) were sequentially injected with three interval measurements. The mean of three measurements was used for further calculations. At the end of the measurement, DNA content of each well was measured using CyQUANT Cell Proliferation Assay kit (Life Technologies). NE-stimulated uncoupled respiration was calculated by subtraction of the oligomycin response values. For normalization, oxygen consumption rate values were divided by the relative DNA content of the corresponding well.

RNA isolation and gene expression analysis

Pulverized fat tissue lysis was performed in QIAzol (Qiagen), and RNA was extracted using RNeasy Mini Kit (Qiagen). RNA from cell lysate in QIAzol was extracted using RNeasy Micro Kit (Qiagen). Complementary DNA was synthesized from 0.1 to 1 μg of total RNA and oligo(dT) primers using SuperScript II (Life Technologies). qPCR was performed using gene-specific TaqMan probes (Life Technologies), diluted in TaqMan Universal Master Mix II or self-designed primers (table S1) with SYBR Green. The application was completed on a

StepOnePlus machine and analyzed by StepOne software v2.3 (Life Technologies). Individual mRNA expression levels were calculated with the $\Delta\Delta C_t$ method and normalized to the expression of TATA-binding protein (murine *Tbp*; human *TBP*) with the exception of the hMADS experiments (which was normalized to *RPLP0*, which encodes ribosomal protein lateral stalk subunit P0, also known as 36B4).

Microarray expression profiling

Acquisition and derivation of mean average signal for each probe on the Illumina Mouse Sentrix-6 BeadChip arrays (Illumina) were performed as previously described (*18*). Intensity values were normalized by quantile normalization using Chipster Software (CSC). GSEA (*25*) was performed on the complete probe data set based on the MouseWG-6_V2_R3_11278593_A annotation. The following gene set collections from the Molecular Signatures Database (MSigDB; www.broadinstitute.org/gsea/msigdb/index.jsp) were used: the c2.cp.kegg.v4.0.symbols.gmt gene set collection, derived from www.genome.jp/kegg/pathway.html, and the c3.tft.v4.0.symbols.gmt gene set collection, in which gene sets contain genes that share a transcription factor binding site defined in the TRANSFAC database (www.gene-regulation.com/). Gene sets were ranked by the false discovery rate.

DNA content analysis

Cells were trypsinized; pelleted; resuspended in D-PBS, 5% FCS (Life Technologies), 0.1% NP-40, and propidium iodide (25 μg/ml; Sigma-Aldrich); and analyzed by flow cytometry on a FACSCalibur (BD Biosciences).

EdU incorporation assay

After 1 hour of incubation with 10 μM EdU, cells were trypsinized and collected, fixed in 4% paraformaldehyde for 15 min, permeabilized, and labeled with Alexa Fluor 647 using the Click-iT Plus EdU Flow Cytometry Assay Kit (Life Technologies). The labeled cells were stained with FxCycle PI/RNase Staining Solution (Life Technologies) and analyzed on a FACSCanto (BD Biosciences).

Immunofluorescence

Cells were fixed with 4% paraformaldehyde (Fisher Scientific) for 10 min, permeabilized with 5% acetic acid in ethanol (100%) for 10 min at −20°C, and blocked with 5% BSA (Sigma-Aldrich) for 1 hour at room temperature. The incubation with anti-Ucp1 primary antibody (1:500; PA1-24894, Thermo Fisher Scientific) in blocking buffer was performed overnight at 4°C. The goat anti-rabbit secondary antibody conjugated with Alexa Fluor 488 was purchased from Invitrogen. The lipid droplets were stained with HCS LipidTOX Red Neutral Lipid Stain (1:500; Life Technologies) in PBS, combined with DAPI (500 ng/ml), to label the cell nuclei for 30 min at room temperature protected from light. Fluorescence microscopy was performed using a motorized Cell Observer Z1 microscope (Zeiss), equipped with the HXP 120 burner, the standard excitation and emission filters for visualizing DAPI (Zeiss filter 49), LipidTox (Zeiss 43 HE Cy3/DsRed), Alexa Fluor 488 (36HE), and AxioCam MRm charge-coupled device camera. Forty-five images were captured randomly across the wells per one condition using the 10×/0.3 PlnN Ph1 DICI objective and ZEN software (Zeiss). All the microscope settings were kept constant during the acquisition, and the measurement of

Ucp1 intensity was performed automatically with constant settings using an ImageJ macro (http://rsbweb.nih.gov/ij). Briefly, nuclei were segmented and counted, and Ucp1 and LipidTox intensity were measured. Nonspecific background was subtracted on the basis of the control samples stained only with secondary antibody. The intensity of Ucp1 signal was normalized to the number of nuclei per field or to the intensity of LipidTox from the same field.

Immunoblotting

Cells were collected in a modified radioimmunoprecipitation assay buffer [150 mM NaCl, 50 mM tris-HCl (pH 8.0), 1% Triton X-100, 0.5% Na deoxycholate, 0.1% SDS, and 1× phosphatase inhibitor and protease inhibitor (cOmplete and PhosSTOP Roche)]. Total protein was extracted by 30-min incubation on ice and subsequent centrifugation at 4°C, 13,000 rpm for 20 min. Pulverized mouse perigonadal fat (100 mg) was lysed in 200 μl of lysis buffer A [50 mM tris (pH 7.4), 1 mM EDTA (pH 8.0), 1.5 mM $MgCl_2$, 10 mM NaF, 2 mM Na_3VO_4, 1 mM dithiothreitol, and 1× protease inhibitor and phosphatase inhibitor (Roche)] using metal beads in a TissueLyser (Qiagen) for 30 s. The lysate was kept on ice for 1 hour, and the separated lower layer was transferred into new tubes. Buffer B (22 μl; 1.5 M NaCl, 5% deoxycholic acid, 10% NP-40, 1% SDS, and 10% glycerol) was added. The procedure was completed by hard shaking at 4°C for 1 hour on a ThermoMixer. The soluble protein fraction was collected after centrifugation at 13,000 rpm for 30 min at 4°C. The amount of protein was measured by BCA kit (Thermo Fisher Scientific), and equal amount of protein was loaded on SDS–polyacrylamide gel electrophoresis. After transferring to nitrocellulose membrane, the membrane was blocked with 5% milk or BSA in tris-buffered saline + 0.1% Tween 20 for 1 hour at room temperature, incubated with Stat3 primary antibody (1:1000; 124H6; #9139, Cell Signaling), pStat3 [1:1000; Tyr^{705} (3E2); #9138, Cell Signalling], Ucp1 (1:1000; PA1-24894, Thermo Fisher Scientific), UCP1 (1:750; 662045, Calbiochem), β-tubulin (1:2000; T5201, Sigma-Aldrich), Smad3 (1:1000; #9513, Cell Signaling), pSmad3 [1:1000; $Ser^{423/425}$ (C25A9); #9520, Cell Signalling], Smad1 (1:1000; D59D7; #6944, Cell Signaling), pSmad1($Ser^{463/465}$)/pSmad5($Ser^{463/465}$)/pSmad8($Ser^{465/467}$) (1:1000; D5B10; #13820, Cell Signaling), Tgfb3 (1:100; ab15537, Abcam), Jak1 (1:500; #3332, Cell Signaling), Jak2 (1:1000; D2E12; #3230, Cell Signaling), Tgfb1 (1:100; ab92486, Abcam), β-actin (1:5000; AC-15; A5441, Sigma-Aldrich), and VCP (1:10,000; ab11433, Abcam) overnight at 4°C, and goat anti-mouse IgG (H+L)-HRP and goat anti-rabbit IgG (H+L)-HRP (Bio-Rad) 1:10,000 for 1 hour at room temperature. Horseradish peroxidase (HRP) activity was enhanced by ECL reagent (GE Healthcare) and detected on a ChemiDoc XRS+ machine (Bio-Rad) using Image Lab 4.1 software.

Enzyme-linked immunosorbent assay

MACS-isolated progenitors were cultured as above and induced to differentiate in DMEM containing 1% BSA in the presence of adipogenic cocktail, 1 μM $cPGI_2$, and 200 nM JakiI. Cell supernatant was collected at 48 hours and applied to ELISA, following the manufacturer's instructions (EA100647, Tgf-beta3 ELISA Kit, OriGene).

Chromatin immunoprecipitation

ChIP was performed using the EZ-ChIP kit (Millipore 17-371) according to the manufacturer's instructions. Briefly, C3H10T1/2 cells were fixed for 10 min with 1% formaldehyde for cross-linking and subsequently quenched with glycine. Cells were collected

in PBS containing protease inhibitor and lysed in SDS lysis buffer (provided in the kit). Chromatin was fragmented to an optimal size of 200 to 500 bp using a Bioruptor Diagenode sonicator. The following antibodies were used for immunoprecipitation: pStat3 (Tyr^{705}) (D3A7; #9145, Cell Signaling) and hemagglutinin tag as IgG control (C29F4; #3724, Cell Signaling). Antibody/chromatin complexes were precipitated with protein G agarose beads and washed in five steps. The protein/DNA complexes were reverse–cross-linked, purified by spin columns, and used for qPCR along with the de-crosslinked/purified input samples. qPCR was performed using SYBR Green, and primers are listed in table S1. The products were analyzed by agarose gel electrophoresis, and the product abundance relative to input was calculated from the C_t values with the $\Delta\Delta C_t$ method.

Immunohistochemistry

Sections (2 μm) of adipose tissue or Matrigel plugs (fixed in 4% paraformaldehyde and paraffin-embedded) were stained with rabbit anti–phospho-Stat3 (Tyr^{705}) (1:100; D3A7, lot 26; #9145, Cell Signaling Technology) or anti-GFP (1:1000; 2OR-GR011, lot P11051325, Fitzgerald Industries International) and counterstained with hematoxylin on a BOND-MAX (Leica). Slides were scanned using a SCN400 slide scanner (Leica) and analyzed using Tissue IA image analysis software (SlidePath, Leica).

Statistical analysis

Experimental analysis was generally not performed in a blinded manner. Plots depict means ± SEM unless otherwise indicated. Expression data were tested in the log scale for approximation of normality. One-way ANOVA with Tukey post hoc pairwise test, two-way ANOVA with Bonferroni post hoc pairwise test, and two-sided *t* test were applied according to the statistical design and have been indicated in the figure legends. A *P* value of ≤0.05 was considered statistically significant ($^{*,\dagger}P \leq 0.05$, $^{**,\dagger\dagger}P \leq 0.01$, and $^{***,\dagger\dagger\dagger}P \leq 0.005$).

SUPPLEMENTARY MATERIALS

www.sciencesignaling.org/cgi/content/full/11/527/eaai7838/DC1

Fig. S1. Continuous inhibition of Jak1/2 activity disrupts white and beige adipocyte differentiation of defined murine progenitors.

Fig. S2. Jak activity is required for human beige adipocyte differentiation.

Fig. S3. The Jak family of kinases promote progenitor activation and adipogenic commitment before the induction of Pparg and its targets.

Fig. S4. The Jak family of kinases inhibit autocrine and paracrine TGFβ signaling to permit commitment and thermogenic differentiation of adipocyte progenitors.

Fig. S5. Stat3 inhibits TGFβ signaling in progenitors and is required for progenitor differentiation.

Fig. S6. Lipolysis-dependent Jak/Stat3 activation and Tgfb3 regulation at the onset of β-adrenergic–induced adipose tissue remodeling.

Fig. S7. IL-11 triggers the Jak/Stat3-Tgfb3 axis in progenitors and in adipose tissue.

Table S1. Sequence of primers used for qPCR analysis.

REFERENCES AND NOTES

1. ↵
    1. E. Jeffery,
    2. C. D. Church,
    3. B. Holtrup,
    4. L. Colman,
    5. M. S. Rodeheffer

    , Rapid depot-specific activation of adipocyte precursor cells at the onset of obesity. Nat. Cell Biol. 17, 376–385 (2015).

    CrossRefPubMedGoogle Scholar

2. ↵
    1. Y. H. Lee,
    2. A. P. Petkova,
    3. E. P. Mottillo,
    4. J. G. Granneman

    , In vivo identification of bipotential adipocyte progenitors recruited by β3-adrenoceptor activation and high-fat feeding. Cell Metab. 15, 480–491 (2012).

    CrossRefPubMedWeb of ScienceGoogle Scholar

3.
    1. L. Vishvanath,
    2. K. A. MacPherson,
    3. C. Hepler,
    4. Q. A. Wang,
    5. M. Shao,
    6. S. B. Spurgin,
    7. M. Y. Wang,
    8. C. M. Kusminski,
    9. T. S. Morley,
    10. R. K. Gupta

    , Pdgfrβ mural preadipocytes contribute to adipocyte hyperplasia induced by high-fat-diet feeding and prolonged cold exposure in adult mice. Cell Metab. 23, 350–359 (2015).

    Google Scholar

4. ↲
    1. Q. A. Wang,
    2. C. Tao,
    3. R. K. Gupta,
    4. P. E. Scherer

, Tracking adipogenesis during white adipose tissue development, expansion and regeneration. Nat. Med. 19, 1338–1344 (2013).

CrossRefPubMedGoogle Scholar

5. ↲
    1. I. G. Shabalina,
    2. N. Petrovic,
    3. J. M. A. de Jong,
    4. A. V. Kalinovich,
    5. B. Cannon,
    6. J. Nedergaard

, UCP1 in brite/beige adipose tissue mitochondria is functionally thermogenic. Cell Rep. 5, 1196–1203 (2013).

CrossRefPubMedWeb of ScienceGoogle Scholar

6. ↲
    1. M. B. Diaz,
    2. S. Herzig,
    3. A. Vegiopoulos

, Thermogenic adipocytes: From cells to physiology and medicine. Metabolism 63, 1238–1249 (2014).

Google Scholar

7.
    1. L. Sidossis,
    2. S. Kajimura

, Brown and beige fat in humans: Thermogenic adipocytes that control energy and glucose homeostasis. J. Clin. Invest. 125, 478–486 (2015).

CrossRefPubMedGoogle Scholar

8. ↲
    1. L. S. Sidossis,
    2. C. Porter,
    3. M. K. Saraf,
    4. E. Borsheim,
    5. R. S. Radhakrishnan,
    6. T. Chao,
    7. A. Ali,

8. M. Chondronikola,
9. R. Mlcak,
10. C. C. Finnerty,
11. H. K. Hawkins,
12. T. Toliver-Kinsky,
13. D. N. Herndon

, Browning of subcutaneous white adipose tissue in humans after severe adrenergic stress. Cell Metab. 22, 219–227 (2015).

CrossRefPubMedGoogle Scholar

9. ↲
    1. Y. H. Lee,
    2. A. P. Petkova,
    3. J. G. Granneman

, Identification of an adipogenic niche for adipose tissue remodeling and restoration. Cell Metab. 18, 355–367 (2013).

CrossRefPubMedWeb of ScienceGoogle Scholar

10. ↲
    1. Y. Qiu,
    2. K. D. Nguyen,
    3. J. I. Odegaard,
    4. X. Cui,
    5. X. Tian,
    6. R. M. Locksley,
    7. R. D. Palmiter,
    8. A. Chawla

, Eosinophils and type 2 cytokine signaling in macrophages orchestrate development of functional beige fat. Cell 157, 1292–1308 (2014).

CrossRefPubMedWeb of ScienceGoogle Scholar

11. ↲
    1. A. Vegiopoulos,
    2. K. Müller-Decker,
    3. D. Strzoda,
    4. I. Schmitt,
    5. E. Chichelnitskiy,
    6. A. Ostertag,
    7. M. Berriel Diaz,
    8. J. Rozman,
    9. M. Hrabe de Angelis,
    10. R. M. Nüsing,
    11. C. W. Meyer,
    12. W. Wahli,
    13. M. Klingenspor,

14. S. Herzig

, Cyclooxygenase-2 controls energy homeostasis in mice by de novo recruitment of brown adipocytes. Science 328, 1158–1161 (2010).

Abstract/FREE Full TextGoogle Scholar

12. ↲
    1. I. Wernstedt Asterholm,
    2. C. Tao,
    3. T. S. Morley,
    4. Q. A. Wang,
    5. F. Delgado-Lopez,
    6. Z. V. Wang,
    7. P. E. Scherer

, Adipocyte inflammation is essential for healthy adipose tissue expansion and remodeling. Cell Metab. 20, 103–118 (2014).

CrossRefPubMedWeb of ScienceGoogle Scholar

13. ↲
    1. J. J. O'Shea,
    2. D. M. Schwartz,
    3. A. V. Villarino,
    4. M. Gadina,
    5. I. B. McInnes,
    6. A. Laurence

, The JAK-STAT pathway: Impact on human disease and therapeutic intervention. Annu. Rev. Med. 66, 311–328 (2015).

CrossRefPubMedGoogle Scholar

14. ↲
    1. A. J. Richard,
    2. J. M. Stephens

, The role of JAK-STAT signaling in adipose tissue function. Biochim. Biophys. Acta 1842, 431–439 (2014).

CrossRefGoogle Scholar

15. ↲
    1. D. Wang,
    2. Y. Zhou,
    3. W. Lei,
    4. K. Zhang,
    5. J. Shi,
    6. Y. Hu,
    7. G. Shu,

8. J. Song

, Signal transducer and activator of transcription 3 (STAT3) regulates adipocyte differentiation via peroxisome-proliferator-activated receptor gamma (PPARγ). Biol. Cell 102, 1–12 (2010).

CrossRefPubMedWeb of ScienceGoogle Scholar

16. ↲
    1. K. Zhang,
    2. W. Guo,
    3. Y. Yang,
    4. J. Wu

, JAK2/STAT3 pathway is involved in the early stage of adipogenesis through regulating C/EBPβ transcription. J. Cell. Biochem. 112, 488–497 (2011).

CrossRefPubMedGoogle Scholar

17. ↲
    1. R. Babaei,
    2. I. Bayindir-Buchhalter,
    3. I. Meln,
    4. A. Vegiopoulos

, Immuno-magnetic isolation and thermogenic differentiation of white adipose tissue progenitor cells. Methods Mol. Biol. 1566, 37–48 (2017).

Google Scholar

18. ↲
    1. I. Bayindir,
    2. R. Babaeikelishomi,
    3. S. Kocanova,
    4. I. S. Sousa,
    5. S. Lerch,
    6. O. Hardt,
    7. S. Wild,
    8. A. Bosio,
    9. K. Bystricky,
    10. S. Herzig,
    11. A. Vegiopoulos

, Transcriptional pathways in cPGI2-induced adipocyte progenitor activation for browning. Front Endocrinol. 6, 129 (2015).

Google Scholar

19. ↲
    1. J. W. Aiken,
    2. R. J. Shebuski

, *Comparison in anesthetized dogs of the anti-aggregatory and hemodynamic effects of prostacyclin and a chemically stable prostacyclin analog, 6a-carba-PGI2 (carbacyclin). Prostaglandins 19, 629–643 (1980).*

CrossRefPubMedWeb of ScienceGoogle Scholar

20. ↲
    1. L. Pedranzini,
    2. T. Dechow,
    3. M. Berishaj,
    4. R. Comenzo,
    5. P. Zhou,
    6. J. Azare,
    7. W. Bornmann,
    8. J. Bromberg

, Pyridone 6, a pan-Janus–activated kinase inhibitor, induces growth inhibition of multiple myeloma cells. Cancer Res. 66, 9714–9721 (2006).

Abstract/FREE Full TextGoogle Scholar

21. ↲
    1. J.-K. Jiang,
    2. K. Ghoreschi,
    3. F. Deflorian,
    4. Z. Chen,
    5. M. Perreira,
    6. M. Pesu,
    7. J. Smith,
    8. D.-T. Nguyen,
    9. E. H. Liu,
    10. W. Leister,
    11. S. Costanzi,
    12. J. J. O'Shea,
    13. C. J. Thomas

, Examining the chirality, conformation and selective kinase inhibition of 3-((3R,4R)-4-methyl-3-(methyl(7H-pyrrolo[2,3-d]pyrimidin-4-yl)amino)piperidin-1-y l)-3-oxopropanenitrile (CP-690,550). J. Med. Chem. 51, 8012–8018 (2008).

CrossRefPubMedGoogle Scholar

22. ↲
    1. R. A. Ghandour,
    2. M. Giroud,
    3. A. Vegiopoulos,
    4. S. Herzig,
    5. G. Ailhaud,
    6. E.-Z. Amri,
    7. D. F. Pisani

, IP-receptor and PPARs trigger the conversion of human white to brite adipocyte induced by carbaprostacyclin. Biochim. Biophys. Acta 1861, 285–293 (2016).

Google Scholar

23. ↲
    1. A. Moisan,
    2. Y.-K. Lee,
    3. J. D. Zhang,
    4. C. S. Hudak,
    5. C. A. Meyer,
    6. M. Prummer,
    7. S. Zoffmann,
    8. H. H. Truong,
    9. M. Ebeling,
    10. A. Kiialainen,
    11. R. Gérard,
    12. F. Xia,
    13. R. T. Schinzel,
    14. K. E. Amrein,
    15. C. A. Cowan

, White-to-brown metabolic conversion of human adipocytes by JAK inhibition. Nat. Cell Biol. 17, 57–67 (2015).

CrossRefPubMedGoogle Scholar

24. ↲
    1. D. F. Pisani,
    2. M. Djedaini,
    3. G. E. Beranger,
    4. C. Elabd,
    5. M. Scheideler,
    6. G. Ailhaud,
    7. E. Z. Amri

, Differentiation of human adipose-derived stem cells into “brite” (brown-in-white) adipocytes. Front. Endocrinol. 2, 87 (2011).

Google Scholar

25. ↲
    1. A. Subramanian,
    2. P. Tamayo,
    3. V. K. Mootha,
    4. S. Mukherjee,
    5. B. L. Ebert,
    6. M. A. Gillette,
    7. A. Paulovich,
    8. S. L. Pomeroy,
    9. T. R. Golub,

10. E. S. Lander,
11. J. P. Mesirov

, Gene set enrichment analysis: A knowledge-based approach for interpreting genome-wide expression profiles. Proc. Natl. Acad. Sci. U.S.A. 102, 15545–15550 (2005).

Abstract/FREE Full TextGoogle Scholar

26. ↵
    1. R. K. Gupta,
    2. Z. Arany,
    3. P. Seale,
    4. R. J. Mepani,
    5. L. Ye,
    6. H. M. Conroe,
    7. Y. A. Roby,
    8. H. Kulaga,
    9. R. R. Reed,
    10. B. M. Spiegelman

    , Transcriptional control of preadipocyte determination by Zfp423. Nature 464, 619–623 (2010).

    CrossRefPubMedWeb of ScienceGoogle Scholar

27. ↵
    1. M. E. McDonald,
    2. C. Li,
    3. H. Bian,
    4. B. D. Smith,
    5. M. D. Layne,
    6. S. R. Farmer

    , Myocardin-related transcription factor A regulates conversion of progenitors to beige adipocytes. Cell 160, 105–118 (2015).

    CrossRefPubMedGoogle Scholar

28. ↵
    1. H. Nobusue,
    2. N. Onishi,
    3. T. Shimizu,
    4. E. Sugihara,
    5. Y. Oki,
    6. Y. Sumikawa,
    7. T. Chiyoda,
    8. K. Akashi,
    9. H. Saya,
    10. K. Kano

, Regulation of MKL1 via actin cytoskeleton dynamics drives adipocyte differentiation. Nat. Commun. 5, 3368 (2014).

CrossRefPubMedGoogle Scholar

29. ↲
    1. F. Miralles,
    2. G. Posern,
    3. A. I. Zaromytidou,
    4. R. Treisman

, Actin dynamics control SRF activity by regulation of its coactivator MAL. Cell 113, 329–342 (2003).

CrossRefPubMedWeb of ScienceGoogle Scholar

30. ↲
    1. Y. Yang,
    2. D. Chen,
    3. Z. Yuan,
    4. F. Fang,
    5. X. Cheng,
    6. J. Xia,
    7. M. Fang,
    8. Y. Xu,
    9. Y. Gao

, Megakaryocytic leukemia 1 (MKL1) ties the epigenetic machinery to hypoxia-induced transactivation of endothelin-1. Nucleic Acids Res. 41, 6005–6017 (2013).

CrossRefPubMedWeb of ScienceGoogle Scholar

31. ↲
    1. C. R. Evelyn,
    2. S. M. Wade,
    3. Q. Wang,
    4. M. Wu,
    5. J. A. Iñiguez-Lluhí,
    6. S. D. Merajver,
    7. R. R. Neubig

, CCG-1423: A small-molecule inhibitor of RhoA transcriptional signaling. Mol. Cancer Ther. 6, 2249–2260 (2007).

Abstract/FREE Full TextGoogle Scholar

32. ↲
    1. C. P. Mack

, *Signaling mechanisms that regulate smooth muscle cell differentiation. Arterioscler. Thromb. Vasc. Biol. 31, 1495–1505 (2011).*

Abstract/FREE Full TextGoogle Scholar

33. ↲
    1. A. Moustakas,
    2. C.-H. Heldin

, Dynamic control of TGF-β signaling and its links to the cytoskeleton. FEBS Lett. 582, 2051–2065 (2008).

CrossRefPubMedWeb of ScienceGoogle Scholar

34. ↲
    1. G. J. Inman,
    2. F. J. Nicolás,
    3. J. F. Callahan,
    4. J. D. Harling,
    5. L. M. Gaster,
    6. A. D. Reith,
    7. N. J. Laping,
    8. C. S. Hill

, SB-431542 is a potent and specific inhibitor of transforming growth factor-β superfamily type I activin receptor-like kinase (ALK) receptors ALK4, ALK5, and ALK7. Mol. Pharmacol. 62, 65–74 (2002).

Abstract/FREE Full TextGoogle Scholar

35. ↲
    1. S. Aparicio-Siegmund,
    2. J. Sommer,
    3. N. Monhasery,
    4. R. Schwanbeck,
    5. E. Keil,
    6. D. Finkenstädt,
    7. K. Pfeffer,
    8. S. Rose-John,
    9. J. Scheller,
    10. C. Garbers

, Inhibition of protein kinase II (CK2) prevents induced signal transducer and activator of transcription (STAT) 1/3 and constitutive STAT3 activation. Oncotarget 5, 2131–2148 (2014).

CrossRefPubMedGoogle Scholar

36. ↲
    1. Z. Wen,
    2. J. E. Darnell Jr.

, Mapping of Stat3 serine phosphorylation to a single residue (727) and evidence that serine phosphorylation has no influence on DNA binding of Stat1 and Stat3. Nucleic Acids Res. 25, 2062–2067 (1997).

CrossRefPubMedWeb of ScienceGoogle Scholar

37. ↲
    1. J. Himms-Hagen,
    2. J. Cui,
    3. E. Danforth Jr.,
    4. D. J. Taatjes,
    5. S. S. Lang,
    6. B. L. Waters,
    7. T. H. Claus

, Effect of CL-316,243, a thermogenic beta 3-agonist, on energy balance and brown and white adipose tissues in rats. Am. J. Physiol. 266, R1371–R1382 (1994).

PubMedWeb of ScienceGoogle Scholar

38. ↲
    1. A. Kosteli,
    2. E. Sugaru,
    3. G. Haemmerle,
    4. J. F. Martin,
    5. J. Lei,
    6. R. Zechner,
    7. A. W. Ferrante Jr.

, Weight loss and lipolysis promote a dynamic immune response in murine adipose tissue. J. Clin. Invest. 120, 3466–3479 (2010).

CrossRefPubMedWeb of ScienceGoogle Scholar

39. ↲
    1. E. P. Mottillo,
    2. X. J. Shen,
    3. J. G. Granneman

, Role of hormone-sensitive lipase in β-adrenergic remodeling of white adipose tissue. Am. J. Physiol. Endocrinol. Metab. 293, E1188–E1197 (2007).

CrossRefPubMedWeb of ScienceGoogle Scholar

40. ↲
    1. E. P. Mottillo,
    2. X. J. Shen,
    3. J. G. Granneman

, β3-adrenergic receptor induction of adipocyte inflammation requires lipolytic activation of stress kinases p38 and JNK. Biochim. Biophys. Acta 1801, 1048–1055 (2010).

PubMedWeb of ScienceGoogle Scholar

41. ↲
    1. G. Schoiswohl,
    2. M. Stefanovic-Racic,
    3. M. N. Menke,
    4. R. C. Wills,
    5. B. A. Surlow,
    6. M. K. Basantani,
    7. M. T. Sitnick,
    8. L. Cai,
    9. C. F. Yazbeck,
    10. D. B. Stolz,
    11. T. Pulinilkunnil,
    12. R. M. O'Doherty,
    13. E. E. Kershaw

    , Impact of reduced ATGL-mediated adipocyte lipolysis on obesity-associated insulin resistance and inflammation in male mice. Endocrinology 156, 3610–3624 (2015).

    CrossRefPubMedGoogle Scholar

42. ↲
    1. S. L. Buzelle,
    2. R. E. MacPherson,
    3. W. T. Peppler,
    4. L. Castellani,
    5. D. C. Wright

    , The contribution of IL-6 to beta 3 adrenergic receptor mediated adipose tissue remodeling. Physiol. Rep. 3, e12312 (2015).

    Abstract/FREE Full TextGoogle Scholar

43.
    1. C. Garbers,
    2. H. M. Hermanns,
    3. F. Schaper,
    4. G. Müller-Newen,
    5. J. Grötzinger,
    6. S. Rose-John,
    7. J. Scheller

    , Plasticity and cross-talk of interleukin 6-type cytokines. Cytokine Growth Factor Rev. 23, 85–97 (2012).

    CrossRefPubMedWeb of ScienceGoogle Scholar

44. ↲
1. V. Mohamed-Ali,
2. L. Flower,
3. J. Sethi,
4. G. Hotamisligil,
5. R. Gray,
6. S. E. Humphries,
7. D. A. York,
8. J. Pinkney

, β-Adrenergic regulation of IL-6 release from adipose tissue: In vivo and in vitro studies. J. Clin. Endocrinol. Metab. 86, 5864–5869 (2001).

CrossRefPubMedWeb of ScienceGoogle Scholar

45. ↲
1. J. Ohsumi,
2. K. Miyadai,
3. I. Kawashima,
4. H. Ishikawa-Ohsumi,
5. S. Sakakibara,
6. K. Mita-Honjo,
7. Y. Takiguchi

, Adipogenesis inhibitory factor. A novel inhibitory regulator of adipose conversion in bone marrow. FEBS Lett. 288, 13–16 (1991).

CrossRefPubMedGoogle Scholar

46. ↲
1. M. Derecka,
2. A. Gornicka,
3. S. B. Koralov,
4. K. Szczepanek,
5. M. Morgan,
6. V. Raje,
7. J. Sisler,
8. Q. Zhang,
9. D. Otero,
10. J. Cichy,
11. K. Rajewsky,
12. K. Shimoda,
13. V. Poli,
14. B. Strobl,
15. S. Pellegrini,
16. T. E. Harris,
17. P. Seale,
18. A. P. Russell,
19. A. J. McAinch,
20. P. E. O'Brien,
21. S. R. Keller,
22. C. M. Croniger,

23. T. Kordula,
24. A. C. Larner

, Tyk2 and Stat3 regulate brown adipose tissue differentiation and obesity. Cell Metab. 16, 814–824 (2012).

CrossRefPubMedGoogle Scholar

47. ↲
    1. P. Hallenborg,
    2. M. Siersbæk,
    3. I. Barrio-Hernandez,
    4. R. Nielsen,
    5. K. Kristiansen,
    6. S. Mandrup,
    7. L. Grøntved,
    8. B. Blagoev

, MDM2 facilitates adipocyte differentiation through CRTC-mediated activation of STAT3. Cell Death Dis. 7, e2289 (2016).

Google Scholar

48. ↲
    1. Y.-H. Tseng,
    2. E. Kokkotou,
    3. T. J. Schulz,
    4. T. L. Huang,
    5. J. N. Winnay,
    6. C. M. Taniguchi,
    7. T. T. Tran,
    8. R. Suzuki,
    9. D. O. Espinoza,
    10. Y. Yamamoto,
    11. M. J. Ahrens,
    12. A. T. Dudley,
    13. A. W. Norris,
    14. R. N. Kulkarni,
    15. C. R. Kahn

, New role of bone morphogenetic protein 7 in brown adipogenesis and energy expenditure. Nature 454, 1000–1004 (2008).

CrossRefPubMedWeb of ScienceGoogle Scholar

49. ↲
    1. H. Yadav,
    2. C. Quijano,
    3. A. K. Kamaraju,
    4. O. Gavrilova,
    5. R. Malek,

6. W. Chen,
7. P. Zerfas,
8. D. Zhigang,
9. E. C. Wright,
10. C. Stuelten,
11. P. Sun,
12. S. Lonning,
13. M. Skarulis,
14. A. E. Sumner,
15. T. Finkel,
16. S. G. Rane

, Protection from obesity and diabetes by blockade of TGF-β/Smad3 signaling. Cell Metab. 14, 67–79 (2011).

CrossRefPubMedWeb of ScienceGoogle Scholar

50. ↵
    1. A. Vegiopoulos,
    2. M. Rohm,
    3. S. Herzig

, Adipose tissue: Between the extremes. EMBO J. 36, 1999–2017 (2017).

Abstract/FREE Full TextGoogle Scholar

51. ↵
    1. M. Ahmadian,
    2. M. J. Abbott,
    3. T. Tang,
    4. C. S. Hudak,
    5. Y. Kim,
    6. M. Bruss,
    7. M. K. Hellerstein,
    8. H. Y. Lee,
    9. V. T. Samuel,
    10. G. I. Shulman,
    11. Y. Wang,
    12. R. E. Duncan,
    13. C. Kang,
    14. H. S. Sul

, Desnutrin/ATGL is regulated by AMPK and is required for a brown adipose phenotype. Cell Metab. 13, 739–748 (2011).

CrossRefPubMedWeb of ScienceGoogle Scholar

52.
    1. E. P. Mottillo,
    2. P. Balasubramanian,
    3. Y.-H. Lee,

4. C. Weng,
5. E. E. Kershaw,
6. J. G. Granneman

, Coupling of lipolysis and de novo lipogenesis in brown, beige, and white adipose tissues during chronic β3-adrenergic receptor activation. J. Lipid Res. 55, 2276–2286 (2014).

Abstract/FREE Full TextGoogle Scholar

53. ↲
    1. E. P. Mottillo,
    2. A. E. Bloch,
    3. T. Leff,
    4. J. G. Granneman

, Lipolytic products activate peroxisome proliferator-activated receptor (PPAR) α and δ in brown adipocytes to match fatty acid oxidation with supply. J. Biol. Chem. 287, 25038–25048 (2012).

Abstract/FREE Full TextGoogle Scholar

54. ↲
    1. D. Sánchez-Infantes,
    2. R. Cereijo,
    3. M. Peyrou,
    4. I. Piquer-Garcia,
    5. J. M. Stephens,
    6. F. Villarroya

, Oncostatin m impairs brown adipose tissue thermogenic function and the browning of subcutaneous white adipose tissue. Obesity 25, 85–93 (2017).

Google Scholar

55. ↲
    1. J. Eguchi,
    2. X. Wang,
    3. S. Yu,
    4. E. E. Kershaw,
    5. P. C. Chiu,
    6. J. Dushay,
    7. J. L. Estall,
    8. U. Klein,
    9. E. Maratos-Flier,
    10. E. D. Rosen

, Transcriptional control of adipose lipid handling by IRF4. Cell Metab. 13, 249–259 (2011).

CrossRefPubMedWeb of ScienceGoogle Scholar

56. ↲

1. C. Elabd,
2. C. Chiellini,
3. M. Carmona,
4. J. Galitzky,
5. O. Cochet,
6. R. Petersen,
7. L. Pénicaud,
8. K. Kristiansen,
9. A. Bouloumié,
10. L. Casteilla,
11. C. Dani,
12. G. Ailhaud,
13. E.-Z. Amri

, Human multipotent adipose-derived stem cells differentiate into functional brown adipocytes. Stem Cells 27, 2753–2760 (2009).

CrossRefPubMedWeb of ScienceGoogle Scholar

57. ↲
    1. A.-M. Rodriguez,
    2. C. Elabd,
    3. F. Delteil,
    4. J. Astier,
    5. C. Vernochet,
    6. P. Saint-Marc,
    7. J. Guesnet,
    8. A. Guezennec,
    9. E.-Z. Amri,
    10. C. Dani,
    11. G. Ailhaud

    , Adipocyte differentiation of multipotent cells established from human adipose tissue. Biochem. Biophys. Res. Commun. 315, 255–263 (2004).

    CrossRefPubMedWeb of ScienceGoogle Scholar

Acknowledgments: We thank S. Boos, J. Hetzer, D. Heide, and T. Sijmonsma for technical assistance (DKFZ); A. Zeilfelder, M. Schilling, and S. Mohapatra (DFKZ) for reagents; S. Henze and O. Heil for microarray experiment support (DKFZ Genomics and Proteomics Core Facility); K. Hexel and S. Schmitt for cell sorting (DKFZ Imaging and Cytometry Core Facility); T. Holland-Letz (DKFZ) for statistics; C. Garbers (Christian-Albrechts-University, Kiel) and F. Rösl (DKFZ) for plasmids; and J. Brüning and T. Wunderlich for valuable discussions (Max Planck Institute Cologne). **Funding:** This work was supported by the Deutsche Forschungsgemeinschaft (HE 3260/8-1), the Helmholtz Association (“Metabolic Dysfunction”), the Human Frontier Science Program (RGY0082/2014), the Young Teacher Research Program of China Scholarship Council, and an NIH grant (R01DK090166 to E.E.K.). **Author contributions:** Conceptualization: R.B., S.H., and A.V.; investigation: R.B., M.S., I.M., R.A.G., D.F.P., I.B.-B., S.W., G.S., J.M., S.L., E.E.K., Y.-H.L., and M.H.; resources: A.T.B., J.M., E.E.K., L.F., B.P.M.-S., and M.H.; software: D.K.; funding acquisition: S.H. and A.V.; supervision: J.G.G., E.-Z.A., E.E.K., S.H., and A.V.; writing: R.B. and A.V. **Competing interests:** The authors declare that they have

no competing interests. **Data and materials availability:** Microarray data are available at Array Express (E-MTAB-6029 and E-MTAB-3693). All other data needed to evaluate the conclusions in the paper are present in the paper or the Supplementary Materials. A material transfer agreement is in place for plasmid pRc/CMV-Stat3-Y705F.